An-Najah National University

Faculty of Graduate Studies

Structural, Electronic and Magnetic Properties of $Al_{1-x}V_xP$ Alloys in Zincblende Structure Using FP-LAPW Method

By

Eman Mohammad Abdelhafeez Al-Rabi

Supervisor
Dr. Mohammed Salameh Salem Abu-Jafar
Co- Supervisor
Dr. Abdel-Rahman Mustafa Abu-Labdeh

This Thesis is Submitted in Partial Fulfillment of the Requirements for the Degree of Master of Science in Physics , Faculty of Graduate Studies, An-Najah National University, Nablus, Palestine.

2012

Structural, Electronic and Magnetic Properties of $Al_{1-x}V_xP$ Alloys in Zincblende Structure Using FP-LAPW Method

By
Eman Mohammad Abdelhafeez Al-Rabi

This thesis was defended successfully on 10 /5/2012 and approved by:

Defense Committee Members		**Signature**
1- Dr. Mohammed Abu- Jafar	**(Supervisor)**	.....
2- Dr. Abdel-Rahman Abu-Labdeh	**(Co-Supervisor)**	.....
3- Prof. Dr. Mohammad M. Abu-Samreh	**(External Examiner)**	.....
4- Dr. Musa El-Hasan	**(Internal Examiner)**	.....

Dedication

To my lovely Father and Mother

To my brothers and sisters

To my husband

With respect

Acknowledgment

I would like to take this opportunity to express my gratitude to the people who provided me their support all long my master study, and thus enabled me to concentrate on my work.

I would like express my sincerely thanks to supervisors Dr. Mohammed Abu- Jafar and Dr. Abdel-Rahman Abu-Labdeh for their advice and support during this work.

Thanks and appreciation are extended to my committee members Prof. Mohammad M. Abu-Samreh (Al-Quds University) as an external examiner and Dr. Musa El-Hasan (An-Najah National University) as an internal examiner for their time and patient.

Finally. I would like also to thank An-Najah University providing all the required resources and support to finish my thesis.

اقرار

انا الموقع ادناه مقدم الرسالة التي تحمل العنوان :

Structural, Electronic and Magnetic Properties of $Al_{1-x}V_xP$ Alloys in Zincblende Structure Using FP-LAPW Method:

اقر بأن ما اشتملت عليه هذه الرسالة انما هو نتاج جهدي الخاص، باستثناء ما تمت الاشارة اليه حيث ورد، وان هذه الرسالة ككل، او أي جزء منها لم يقدم من قبل لنيل اية درجة او لقب علمي او بحث لدى مؤسسة تعليمية او بحثية اخرى.

Declaration

The work provided in this thesis, unless otherwise referenced, is the researcher's own work, and has not been submitted elsewhere for any other degree or qualification.

Student's name: **اسم الطالب:**

Signature : **التوقيع :**

Date : **التاريخ :**

Table of Contents

List of Tables

List of Figures

Structural, Electronic and Magnetic Properties of $Al_{1-x}V_xP$ Alloys in Zincblende Structure Using FP-LAPW Method

By

Eman Mohammad Abdelhafeez Al-Rabi

Supervisors

Dr. Mohammed S. Abu-Jafar

Co-Supervisor

Dr. Abdel-Rahman M. Abu-Labdeh

Abstract

In this study, the structural, electronic and magnetic properties of $Al_{1-x}V_xP$ alloys, with concentration x = 0, 0.125, 0.25, 0.5, 0.75 and 1 in zincblende structure (ZB) are calculated, using self consistent full potential linearized augmented plane wave (FP-LAPW) method, implemented by the WIEN2k code, with local spin density approximation (LSDA) and generalized gradient approximation (GGA) for the energy and the exchange correlation potential.

The evolution of band structure and magnetic moment were studied as a function of the lattice parameter of the AlP compound and the ternary alloys $Al_{1-x}V_xP$ with x= 0.125, 0.25, 0.5, 0.75 and 1. The obtained results are in good agreement with experimental results and other theoretical calculations.

It is found that AlP is semiconductor, having an indirect band gap energy of approximately 1.6 eV using LSDA method with an almost zero magnetic moment for ZB structure.

At x=0.125, the AlP semiconductor has an indirect energy gap of 0.3 eV.

For the ternary alloys $Al_{1-x}V_xP$ with x= 0.25, 0.5 and 0.75, the energy band gap is zero, such results characterize metal or semimetal compounds. The total magnetic moment for these ternary alloys depend on the concentration of V, while VP compound has shown the metal character with a total magnetic moment of 2 Bohr magneton (μ_B) / unit cell.

The total energy dependence on the lattice constant is obtained using the spin density functional theory (DFT). It was found that the lattice parameter depends directly with the concentration of V.

It was also found that on the Contrary to the bulk modulus and energy, values of the lattice parameter, total magnetic moments and energy band gap obtained using GGA method are larger than that using LSDA method.

Chapter 1
Introduction

Semiconductors are widely used in most technological fields. They can be found either in group IV elements, such as silicon (Si) and germanium (Ge) , or in group III-V and II-IV compounds.

An important example of group III-V semiconductors is aluminum phosphide (AlP); which has zincblende (ZB) structure at ambient condition with lattice constant $a_0 = 5.4635$ angstrom (Å) [1]; but at high pressure it undergoes a transition to nickel arsenide (NiAs) structure [2]. In ZB structure, it was found that this compound is unstable in air [1], and it has an indirect band gap energy $E_g = 2.505$ eV [3]. In addition, it emits poisonous phosphine gas at high pressure, which makes its experimental study too difficult and unique to be performed [4,5]. At 19 Gpa, AlP has a NiAs (hexagonal) structure with lattice constants $a_0 = 3.466$ Å and $c = 5.571$ Å [2]. Moreover, this compound is used in optoelectronic device application in the visible range [6].

Theoretical investigation on AlP. Saeed *et al* [7] studied this compound in ZB structure by using full potential linearized augmented plane wave plus local (FP-LAPW+lo) with local spin density (LSDA) approximation. It was found that its lattice constant is about $a_0 = 5.434$ Å and its bulk modulus (B_0) is about 85.5 gigapascal (GPa). On the other hand, Kulkova *et al* [8] have been studied its structural and electronic properties in the ZB structure using FP-LAPW method within local density approximation

(LDA). They obtained the following physical parameters: $a_0 = 5.44\,\text{Å}$, $B_0 = 95.5$ GPa and $E_g^{ID} = 1.45$ eV. In another investigation. The electronic properties of this compound using FP-LAPW method within LDA approximation has been performed by Reshak *et al* [9] and an energy gap of $E_g^{ID} = 1.49$ eV is obtained.

Annane *et al* [10] were used FP-LAPW+lo method within PW-GGA approximation to study ZB structure of this compound. The obtained results are $a_0 = 5.507\,\text{Å}$, $B_0 = 82.619$ GPa and $E_g^{ID} = 1.632$ eV. Moreover, Yu *et al* [11] were studied AlP compound using FP-LAPW+lo method within GGA approximation in ZB structure to explore its structural and electronic properties. It was found that $a_0 = 5.508\,\text{Å}$, $B_0 = 81.52$ GPa and $E_g^{ID} = 1.635$ eV. Briki *et al* [12] also investigated AlP compound in ZB structure using the FP-LAPW method within local density approximation (LDA) as well as general gradient approximation (GGA). They have pointed out that $a_0 = 5.44\,\text{Å}$, $B_0 = 90.9$ GPa using LDA approximation, while $a_0 = 5.52\,\text{Å}$, $B_0 = 83.2$ GPa using GGA approximation. They also found using Engel-Vosko (EV-GGA) approximation that $E_g^{ID} = 2.49$ eV. Within the same method Ahmed *et al* [13] predicted that $a_0 = 5.436\,\text{Å}$, $B_0 = 89$ GPa and $E_g^{ID} = 1.44$ eV using LDA approximation, and $a_0 = 5.511\,\text{Å}$, $B_0 = 82$ GPa and $E_g^{ID} = 1.57$ eV using GGA approximation.

The pseudopotential method has performed by Mujica *et al* [14] to study AlP compound in ZB structure within LDA approximation for exchange correlation potential. They found that $V_0 = 39.91\,(\text{Å})^3$

($a_0 = 5.42$ Å), $B_0 = 90$ GPa. In addition, Froyen *et al* [15] used the pseudopotential total energy scheme within LDA approximation in ZB structure for AlP compound to investigate the structural properties. The obtained results were $a_0 = 5.42$ Å, $B_0 = 86.5$ GPa. Wang *et al* [16] also used plane wave pseudopotential approximation within LDA approximation by using the Hartwigsen-Goedeccker-Hutter relativistic seperable dual-space Gaussian pseudopotentials to find the structural properties for AlP compound in ZB structure. They showed that $a_0 = 5.417$ Å, $B_0 = 88.6$ GPa. Indeed, Zhang *et al* [17] used the pseudopotential total energy approach using the method of Hamann, Schülter and Chiang with the modification introduced by Kleinman to investigate the structural properties for AlP in ZB structure. They found that $a_0 = 5.471$ Å, $B_0 = 84.5$ GPa. Moreover, Rodríguez-Hernándes *et al* [18] used an ab initio pseudopotential calculation within LDA approximation in ZB structure to find the structural properties. They found that $a_0 = 5.4$ Å, $B_0 = 90$ GPa.

AlP has also been studied by Arbouche *et al* [4] in many structures using FP-LAPW+lo within GGA approximation. They found that ZB structure is a ground state with $a_0 = 5.51$ Å, $B_0 = 83.23$ GPa, whereas $a_0 = 3.72$ Å, c/a_0=1.46 and $B_0 = 102.31$ GPa in NiAs structure. On the other hand, Aouadi *et al* [5] studied this compound using pseudopotential method with LDA approximation. It has been found that $a_0 = 5.43$ Å, $B_0 = 90.46$ GPa and $E_g^{ID} = 1.41$ eV in ZB structure, while $a_0 = 3.55$ Å, c = 5.71 Å and $B_0 = 111.5$ GPa in NiAs structure. Chin-Yu Yeh *et al* [19] also studied AlP compund in ZB structure using local density formalism (LDF) within

Ceperley Alder exchange correlation and plane wave non local pseudopotential method. They found that $a_0 = 5.421$ Å. Huang et al [20] used the first principles orthogonalized linear-combination-of-atomic-orbitals (OLCAO) method in LDA approximation to investigate the structural and electronic properties for AlP compound in ZB structure. They showed that $a_0 = 5.462$ Å and $E_g^{ID} = 2.17$ eV.

In this work, vanadium is doped with AlP. Vanadium is in group V with d-shell [21], which makes it a transition metal. Vanadium compounds (VX) have many important properties such as their interesting electrochemical and magnetic properties [21]. An important compound among (VX) compounds is the vanadium phosphide (VP) which was found in nickel arsenide (NiAs) structure with large ratio of lattice parameter c to a_0(c / a_0) [23]. This makes the metal-metal interaction in c direction small. The Hukel method has been employed in studying VP in NiAs structure by Kematick *et al* [23]. They found that $a_0 = 3.18$ Å, c = 6.224 Å (c / a_0=1.956). Moreover, Galanakis et al [24] studied VP in ZB structure. They pointed out that VP has a lattice constant of $a_0 = 5.27$ Å was obtained.

Due to the combination of magnetic and semiconducting properties, doping III-V semiconductors using transition metal (TM) is of great importance to the research groups world. This combination may create some features lead to many applications such as high speed electronic, optoelectronic and spintronic devices [25,26]. These applications require Curie's temperature to be higher than room temperature [27]. This can be

achieved by doping the semiconductor with TM such as Mn-doped AlN [28], Mn-doped GaN [29] and Cr-doped AlN [30,31].

Recently, this type of materials attract attention of researchers worldwide due to the importance of magnetic properties of such alloys and their electronic applications.

In this study, AlP is doped with vanadium ($Al_{1-x}V_X P$) at different concentrations (x= 0, 0.125, 0.25, 0.5, 0.75, 1). The electronic, structural and magnetic properties of $Al_{1-x}V_X P$ for x= 0, 0.125, 0.25, 0.5, 0.75 and 1were investigated. Calculations were performed using FP-LAPW [32] method based on density functional theory (DFT) within LSDA and GGA approximations.

This thesis is organized as follows: Chapter 2 presents a brief reviewed of theoretical background of solids and approximations that can be used in solving Schrodinger equation. In addition, in this chapter, the methodology used in the calculations were presented. Chapter 3, presents the results and calculations for both binary compounds (AlP and VP) and their alloys ($Al_{1-x}V_X P$). Finally, Chapter 4, includes comments from the study and suggestions for future work.

Chapter 2

Density functional theory

2.1 Introduction

Solid contains a huge numbers of molecules or atoms, that is a collection of n negatively charged particles (electrons) and N positively charged particles (nuclei). Therefore, when studying the properties of solids, many body problem should be treated quantum mechanically. It is worth noting that, particles are very light, so that quantum many body problem is imposed [33].

Physical Properties of solids, such as electrical conductivity, thermal conductivity, specific heat, optical and magnetic properties are calculated through the solving time independent Schrödinger equation, thus,

$$\hat{H}\Psi=E\Psi, \tag{2.1}$$

where Ψ is the N-body wave function and $\hat{H}$ is the Hamiltonian of this system, which is given by

$$\hat{H} = -\frac{\hbar^2}{2}\sum_i \frac{\nabla^2_{\vec{R}_i}}{M_e} - \frac{\hbar^2}{2}\sum_i \frac{\nabla^2_{\vec{r}_i}}{m_e} - \frac{1}{4\pi\varepsilon_0}\sum_{i,j}\frac{e^2 Z_i}{\left|\overrightarrow{R_i}-\overrightarrow{r_j}\right|} + \frac{1}{8\pi\varepsilon_0}\sum_{i\neq j}\frac{e^2}{\left|\overrightarrow{r_i}-\overrightarrow{r_j}\right|} + \frac{1}{8\pi\varepsilon_0}\sum_{i\neq j}\frac{e^2 Z_i Z_j}{\left|\overrightarrow{R_i}-\overrightarrow{R_j}\right|}, \tag{2.2}$$

This equation (2.2) can be written as:

$$\hat{H} = \hat{T}_N + \hat{T}_e + \hat{V}_{Ne} + \hat{V}_{ee} + \hat{V}_{NN}. \tag{2.3}$$

The first term of equation (2.2) is the kinetic energy operator of nucleus i ($\hat{T}_N$), where the nucleus i is at position R_i with mass M_i . The second term of equation (2.2) is the kinetic energy operator of electrons ($\hat{T}_e$), where the electron i is at r_i with mass m_e. The last three terms of equation (2.2) are coulomb interactions between nucleus- electron ($\hat{V}_{Ne}$), electron- electron ($\hat{V}_{ee}$) and nucleus- nucleus ($\hat{V}_{NN}$), respectively. Thus, equation (2.2) can be written as

Solving equation (2.3) is complicated because the term ($\hat{V}_{Ne}$) makes the Hamiltonian in equation (2.3) non-separable variables (i.e., we cannot write the wave function as a product of electronic part and nuclear part). Therefore, some approximations are needed to solve equation (2.3). This is discussed in the subsequent sections.

2.2 Born-Oppenheimer Approximation (BOA)

The BOA is based on the fact that nuclei are heavier and slower than electrons ($m_e/M_N \sim 10^{-4}$- 10^{-6}). Therefore, nuclei are assumed to be static at certain positions. This fact leads to vanish the term T_N . and V_{NN} can be considered to be constant. This constant can be removed from Hamiltonian and added it after finishing the calculation, because R_i is now a parameter not a variable.

Based on this approximation, equation (2.3) becomes

$$\hat{H} = \hat{T}_e + \hat{V}_{Ne} + \hat{V}_{ee}. \qquad (2.4)$$

Equation (2.4) shows that the Hamiltonian depending explicitly on electron coordinates and parametrically on nuclear coordinates. Although this approximation reduce the complexity of solving original problem (i. e., equation (2.1), it is still very difficult to solve analytically because the V_{ee} term.

2.3 Density functional theory (DFT)

As mentioned in the previous section, the remaining Hamiltonian still needs some approximation. One of the important approximations is the so called Hartree approximation, where the many electron wave function is considered as a product of a set single electron wave function. However, this assumption disagrees with Pauli exclusive principle. Then, Hartree-Fock inserted additional potential term called an exchange potential [34]. Although Hartree-Fock approximation is a good one for atoms and molecules in general, but it is not accurate enough in the field of solid state physics [33].

2.3.1 Hohenburge Kohn theorems

Another intelligent and more useful approximation that was developed in 1964 by Hohenburge and Kohn [35], and called the density functional theory (DFT), was employed with much success to solve the many body

problem in general . Hohenburge and Kohn showed that the ground state electron density for interacting electrons is one to one function with external potential. In other words, they showed that the external potential is a functional of electron density, with condition of minimizing energy as illustrated by the equation

$$E[\rho] \leq E_0, \tag{2.5}$$

where E_0 is the ground state energy of the system. This type of approximation generally is called variational theory. When ρ is the ground state density (i.e., $\rho = \rho_0$), equation (2.5) can be rewritten as

$$E[\rho_0] = E_0. \tag{2.6}$$

From the assumptions of Hohenburge and Kohn, the total energy of the system can be expressed as

$$\begin{aligned} E[\rho] &= \left\langle \Psi \middle| \hat{T}_e + \hat{V}_{ee} \middle| \Psi \right\rangle + \left\langle \Psi \middle| \hat{V}_{Ne} \middle| \Psi \right\rangle, \\ &= \underbrace{T_e[\rho] + V_{ee}[\rho]}_{F[\rho]} + \int \rho(\vec{r}) \hat{V}_{Ne}(\vec{r}) d\vec{r}, \\ &= F[\rho] + \int \rho(\vec{r}) V_{Ne}(\vec{r}) d\vec{r}, \end{aligned} \tag{2.7}$$

where the density functional $F[\rho]$, which includes the internal energy for interacting system, but independant on nuclei or their positions. Therefore, it can be used for many electron system, which makes it a universal term [33].

It is worth noting that the electron density depends on 3 or 4 variables, while the wave function is a function of 3N variables.

2.3.2 Kohn Sham equation

The complexity of solving Schrodinger equation is in finding $F[\rho]$ exactly. Kohn Sham derive an equation in 1965 [36]. They had assumed non interacting electrons instead of interacting electrons, with the same total electron density (ρ) that it can be found from the equation

$$\rho(\vec{r}) = \sum_{i=1}^{N} \phi_i^*(\vec{r})\phi_i(\vec{r}), \tag{2.8}$$

where ϕ_i is a single electron wave function.

To make a reasonable approximation, a non interacting electron kinetic energy operator ($T_S[\rho]$) should be added to $F[\rho]$. Thus

$$\begin{aligned} F[\rho] &= T_e[\rho] + V_{ee}[\rho] + T_S[\rho] - T_S[\rho] \\ &= T_S[\rho] + V_{ee}[\rho] + (T_e[\rho] - T_S[\rho]) + V_H[\rho] - V_H[\rho] \\ &= T_S[\rho] + V_H[\rho] + \underbrace{(T_e[\rho] - T_S[\rho]) + (V_{ee}[\rho] - V_H[\rho])}_{V_{XC}} \\ &= T_S[\rho] + V_H[\rho] + V_{XC}[\rho], \end{aligned} \tag{2.9}$$

where $V_H[\rho]$ is Hartree potential (classical e-e interaction) and V_{XC} is exchange-correlation potential, which is equal to difference between total energy for interacting and non interacting systems [33]. The physical meaning of $V_{XC}[\rho]$ is equivalent to Pauli exclusive principle. The electrostatic energy for parallel electron spin (anti symmetry) is higher than electrostatic energy for opposite electrons spin (symmetry) and differs from classical (Hartree) electrostatic energy[37]. The Hamiltonian of such system, therefore, becomes

$$\hat{H}_{KS} = \hat{T}_s + \hat{V}_H + \hat{V}_{Ne} + \hat{V}_{XC}$$
$$= -\frac{\hbar}{2m}\nabla_i^2 + \frac{e^2}{4\pi\varepsilon_0}\int \frac{\rho(\vec{r})}{|r-\vec{r}|}d\vec{r} + \int \rho(\vec{r})\hat{V}_{Ne}(\vec{r})d\vec{r} + \frac{\delta V_{XC}[\rho]}{\delta\rho}, \qquad (2.10)$$

where,

$$\hat{H}_{KS}\phi_i = \varepsilon_i\phi_i \qquad (2.11)$$

To solve equation (2.10) and hence calculate V_{Ne} and V_H, require a well known ρ. This can be found according to the flowchart in Figure (2.1), that exhibit the self-consistency with iterative procedure [33].

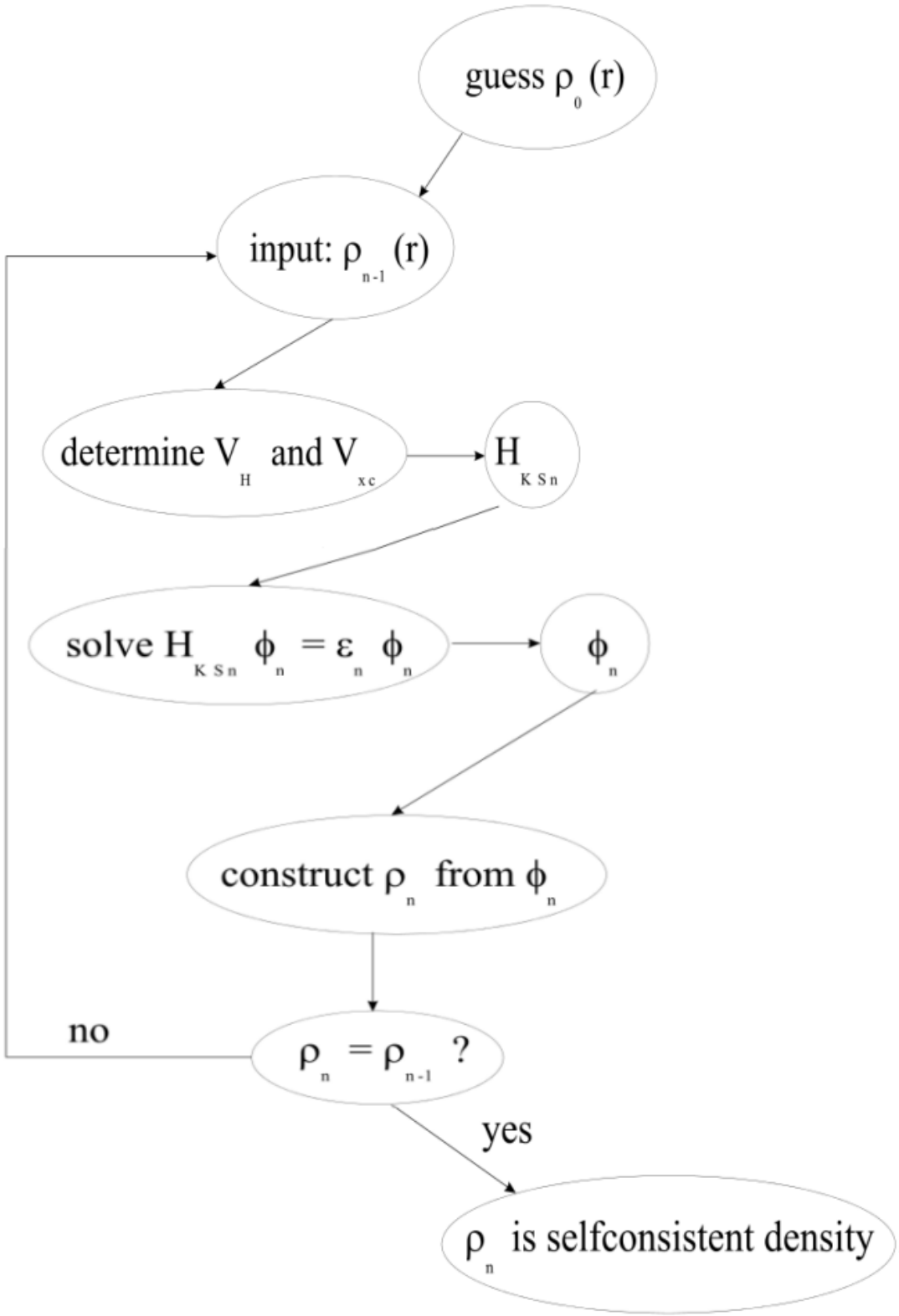

Figure (2.1) : The flowchart of density functional theory.

The last term in equation (2.10), V_{XC}, is calculated using to the local spin density (LSDA) and generalized gradient (GGA) approximations. Both LSDA and GGA approximations are presented and discussed in the following sections.

2.3.3 The local spin density approximation (LSDA)

As mentioned before, some approximations are needed to find V_{XC} potential. One of commonly used approximation is the local spin density approximation (LSDA). The name local is used to indicate that the exchange-correlation potential at r depends only on spin density at r.

In this approximation, the inhomogeneous system is divided into large number of infinitesimal volumes with constant spin density. The exchange-correlation energy for each small volume (ε_{XC}) is equal to the exchange-correlation energy for same volume and spin density in a homogeneous gas system, which can be found by several methods like quantum Monte Carlo method [38]. Therefore, the total energy for such systems can written as [39]:

$$E_{XC}^{LSDA}[\rho(\vec{r})] = \int \rho_{\sigma}(\vec{r})\varepsilon_{XC}(\rho_{\sigma}(\vec{r}))d\vec{r}, \tag{2.12}$$

and

$$V_{XC} = \frac{\delta E_{XC}}{\delta \rho} = \varepsilon_{XC} + \rho\frac{\partial \varepsilon_{XC}}{\partial \rho}, \tag{2.13}$$

where, ρ_{σ} is the total spins, up and down , as shown below

$$\rho_\sigma = \rho_\uparrow + \rho_\downarrow . \qquad (2.14)$$

This method is applicable only to systems which have slow density variation. This restriction resulted in some limitations to the present method [33].

2.3.4 The general gradient approximation (GGA)

Here, the exchange-correlation potential at r depends on the spin density at r and its neighbors such as gradient of spin density. In such approximation, the total energy then gives [40] :

$$E_{XC}^{GGA}[\rho(\vec{r})] = \int \rho_\sigma(\vec{r})\varepsilon_{XC}(\rho_\sigma(\vec{r}))\vec{\nabla}\rho(\vec{r})d\vec{r}, \qquad (2.15)$$

Where $\vec{\nabla}\rho(\vec{r})$ is the gradient of spin density.

2.4 Full potential-linearized augmented plane-wave (FP-LAPW) method

One of the well known methods that can be used to solve Kohen-Sham equation is the variational method. This method is indicated by writing the wave function of the system as a linear combination of plane wave basis with k wave vector in the irreducible Brillouin zone and K reciprocal lattice vector as

$$\psi_K^k = \sum C_K^k e^{i(\vec{k}+\vec{K}).\vec{r}}, \qquad (2.16)$$

This is called Bloch wave function.

Even though, this method is inefficient because the wave function for

electron near to nucleus was varying very quickly. This makes plane wave (PW) converges very slowly and need a large number of wave vectors $(K_{\max})$ to get the accuracy. Therefore, the set up of calculation becomes impossible [41]. The augmented plane-wave (APW) method was suggested by Slater in 1937 [42, 43] to handle such difficulty. He introduced an approximate potential by dividing the unit cell into two regions as seen in Figure (2.2). The first one is the non overlapping sphere (I) with radius R_α, with spherical potential and radial wave function times spherical harmonic function $Y_{l,m}$. The second is interstitial region (II) with constant potential and plane wave function. This method is called Muffin tin (MT) approximation.

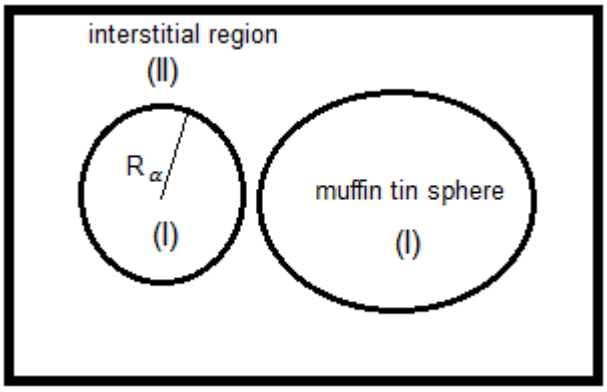

Figure (2.2) : The interstitial and muffin tin sphere region in unit cell at muffin tin approximation.

The bases function in APW are

$$\psi = \begin{cases} \dfrac{1}{\sqrt{V}} e^{i(\vec{k}+\vec{K}).\vec{r}} & \vec{r} \in I \\ \sum A_{l,m}^{\vec{k}+\vec{K}} \upsilon_l(\vec{r}', E) Y_{l,m}(\vec{r}') & \vec{r} \in R_\alpha \end{cases}, \qquad (2.17)$$

where V is the volume of the unit cell, $\vec{r}' = r - r_\alpha$, r_α is the atomic

position within the unit cell and υ_l is radial solution of Schrodinger equation for free atom at energy E. In equation (2.17), $A_{l,m}^{\vec{k}+\vec{K}}$ can be determined by matching a muffin tin (MT) and plane wave. The energy dependent radial function leads to nonlinear eigen value problem and makes the dealing with this method not practical [33,41].

Using Taylor expansion, we can write υ_l in terms of fixed E (E_0) as

$$\upsilon_l(r',E)=\upsilon_l(r',E_o)+(E-E_0)\ \frac{\partial\upsilon_l(r',E)}{\partial E}\Big|_{E=E_o}+O(E_o-E)^2 \qquad (2.18)$$

The linearized APW suggested by Andersen [44]. Substituting $\upsilon_l(r',E)$ in equation (2.17), to obtain:

$$\psi=\begin{cases}\dfrac{1}{\sqrt{V}}e^{i(\vec{k}+\vec{K}).\vec{r}} & \vec{r}\in I\\ \sum A_{l,m}^{\vec{k}+\vec{K}}\upsilon_l(\vec{r}',E_0)+B_{l,m}^{\vec{k}+\vec{K}}\dot{\upsilon}_l(\vec{r}',E_0)Y_{l,m}(\vec{r}') & \vec{r}\in R_\alpha\end{cases}, \qquad (2.19)$$

where $A_{l,m}^{\vec{k}+\vec{K}}$ and $B_{l,m}^{\vec{k}+\vec{K}}$ can be found by matching the plane wave and its derivative at the sphere boundary. This method, however, consider only the charge density of core electrons (i. e., electrons near the nucleus) and ignores the charge density of valence electrons (i. e., electrons far from nucleus such as d or f states). Therefore, a modified method is needed. This method is called LAPW + Lo which introduced by Singh [45] to augmented the LAPW basis set for certain l value. Within this method, equation (2.19) becomes

$$\psi = \begin{cases} 0 & \vec{r} \notin R_\alpha \\ \sum A_{l,m}^{LO} \upsilon_l(\vec{r}', E_1) + B_{l,m}^{LO} \dot{\upsilon}_l(\vec{r}', E_1) + C_{l,m}^{LO} \upsilon_l(\vec{r}', E_2) Y_{l,m}(\vec{r}') & \vec{r} \in R_\alpha \end{cases}, \quad (2.20)$$

where local orbital is zero in the interstitial region and inside muffin tin spheres of other atoms, E_1 is the energy of highest valence state and E_2 is the energy of the lower state. $A_{l,m}$, $B_{l,m}$ and $C_{l,m}$ are obtained by normalizing ψ and must be zero in value and slope at sphere's boundary. The problem in this method is the large size of bases. This can be decreases by APW + lo method (suggested by E.Sjöstedt *et al* [46]) .This method converges faster than LAPW towards the basis set limit with same accurate [47]. Thus, ψ can be written as

$$\psi = \begin{cases} 0 & \vec{r} \notin R_\alpha \\ \sum A_{l,m}^{lo} \upsilon_l(\vec{r}', E_1) + B_{l,m}^{lo} \dot{\upsilon}_l(\vec{r}', E_1) Y_{l,m}(\vec{r}') & \vec{r} \in R_\alpha \end{cases} \quad (2.21)$$

Finally, the full potential LAPW used to deal without any approximation in potential is of the form [32]

$$V = \begin{cases} \sum V_{l,m} Y_{l,m} & \textit{inside sphere} \\ \sum V e^{i\vec{k}.\vec{r}} & \textit{outside sphere} \end{cases} \quad (2.22)$$

Chapter 3

Computational Details, Results and Discussions

3.1 Introduction

In this study, calculations are performed on AlP and VP binary compounds as well as their alloys $Al_{1-x}V_xP$ (x=0.125,0.25,0.5,0.75) using FP-LAPW [32] method within LSDA [39] and GGA [40] approximations based on DFT [35,36] as implemented in WIEN2K 2009 code [47].The maximum value of l, in the wave function expansion inside the atomic sphere, is confined to $l_{\max} = 10$. For the expansion of the wave functions in the interstitial region, the plane wave cutoff energy is $R_{mt}K_{\max}$ (where R_{mt} is the muffin tin radius of atoms in the unit cell and $K_{\max}$ is the maximum modulus for the reciprocal lattice vector). The charge density is expanded up to $G_{\max} = 12$ for LSDA and 16 for GGA. A 20 k points which are taken in the irreducible wedge of the Brillouin zone are used to achieve good and very close convergence of the total energy. A Muffin tin radius for each atom (R_{mt}) must be chosen in certain conditions to avoid possible overlaps between itself and others. In this study, therefore, R_{mt} is set to be 2.0 arbitrary unit (a.u.) for Al and P atoms, and to be 2.1 a.u. for V atom.

The present calculations have investigated the structural, electronic and magnetic properties of each system of interest. Hence, the computational details as well as the calculated results and their discussions are presented in this chapter.

3.2 Atomic positions and structures

In the zincblende (ZB) structure, atoms for each system of interest are ordered in positions to get the total energy of the ground state. Therefore, optimization is performed to minimize the total energy with respect to the atomic position in order to get the desired results as discussed below.

3.2.1 Binary compounds (AlP and VP)

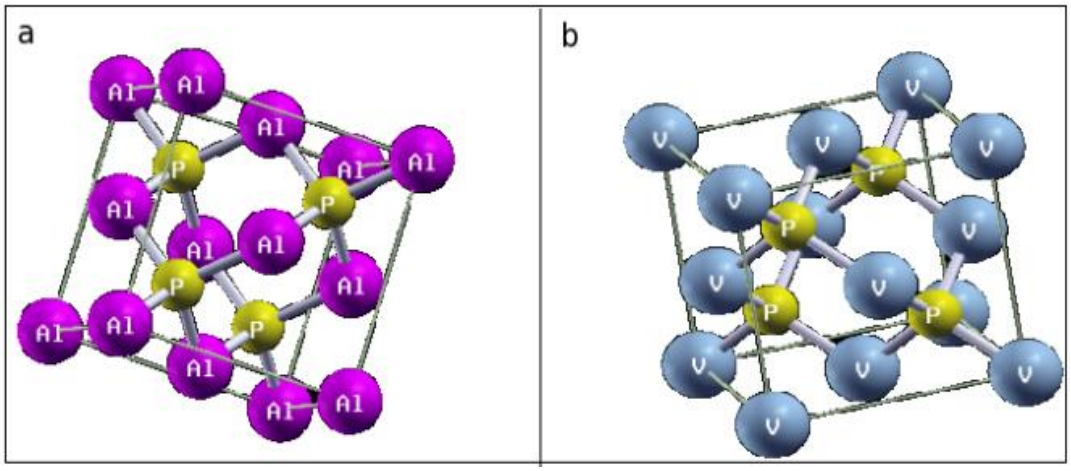

Figure (3.1) : Unit cell used to simulate the $Al_{1-x}V_xP$ alloys in ZB structure (a) x = 0 (i.e., AlP) and (b) x = 1 (i.e., VP).

In this case, both AlP and VP compounds are considered to be ZB structure with space group 216 (F-43m). In AlP compound, the coordinates for Al atom is chosen to be (0,0,0) and for P atom is chosen to be (1/4,1/4,1/4) as shown in Figures (3.1 a). In VP compound, the coordinates for V atom is also chosen to be (0,0,0) and for P atom is chosen to be (1/4,1/4,1/4) as shown in Figures (3.1 b).

The total number of k points is chosen to be 343, which leads to 20 k points in the irreducible Brillouin zone (IBZ) and a Monkhorst – Pack mesh

[48] of 7×7×7 k mesh of points.

Although some researchers showed that the structural ground state of VP compound is NiAs structure [24,49], ZB structure is considered in this study for the purpose of comparison with AlP and its alloys.

3.2.2 $Al_{1-x}V_xP$ alloys at x= 0.25 and 0.75

In this case, ZB structure for $Al_{1-x}V_xP$ alloys when x= 0.25 and 0.75 with space group 215 (P-43m) have been investigated. In $Al_{0.75}V_{0.25}P$, the coordinates of Al, V and P are chosen to be (0,0.5,0.5), (0,0,0) and (1/4,1/4,1/4), respectively, (see Figure 3.2 a). In $Al_{0.25}V_{0.75}P$, the coordinates of Al, V and P are also chosen to be (0,0,0), (0,0.5,0.5) and (1/4,1/4,1/4), respectively. This is shown in Figure (3.2 b).

The number of k points is chosen to be 343, which leads to 20 k points in the IBZ, and 7×7×7 Kmesh.

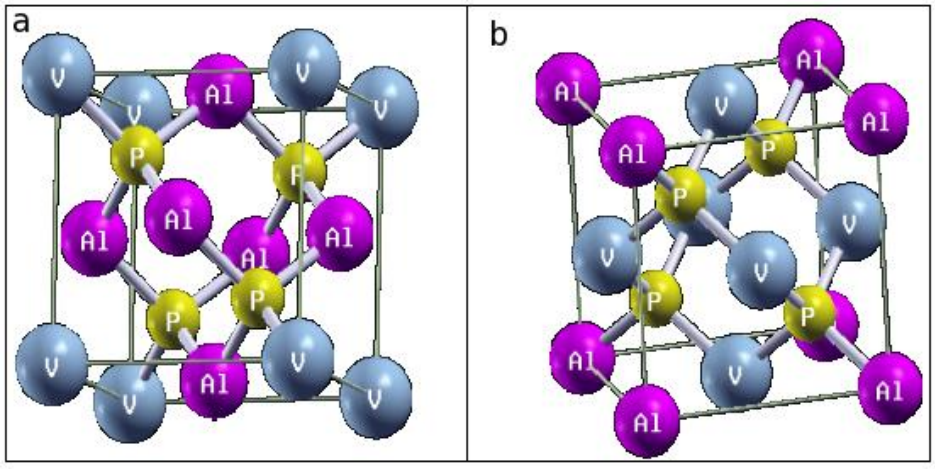

Figure (3.2): Unit cell used to simulate the $Al_{1-x}V_xP$ alloys in ZB structure:
(a) x=0.25 and (b) x=0.75

3.2.3 $Al_{1-x}V_xP$ alloys at x= 0.5

For $Al_{0.5}V_{0.5}P$, ZB structure with space group 111 (P-42m) has been investigated, with 4 atoms. In this alloy, the coordinates are (0,0,0) and (0.5,0.5,0) of Al atoms, (0,0.5,0.5) for V atoms and (1/4,1/4,1/4) for P atoms, as shown in Figure (3.3).

The number of k points is chosen to be 216, which leads to 18 k points in the IBZ, and 6×6×6 Kmesh of points.

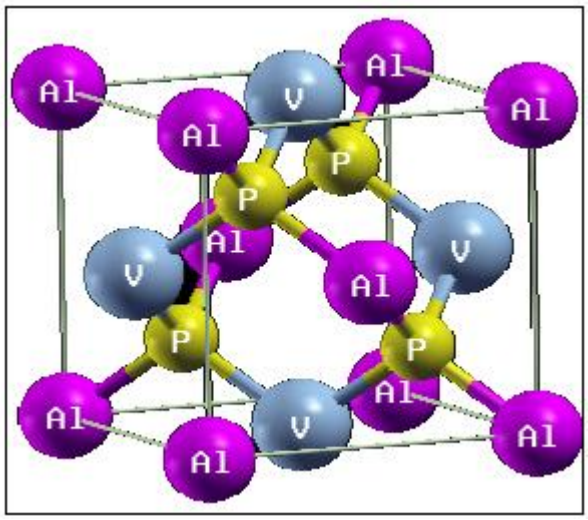

Figure (3.3): Unit cell used to simulate the $Al_{1-x}V_xP$ alloys in ZB structure, x = 0.5.

3.2.4 $Al_{1-x}V_xP$ alloys at x= 0.125

For this alloy, we have used super cell (i. e., we have duplicated the number of unit cells in x direction). In other words, we have used $Al_{1-x}V_xP$ for x=0.25, then we have duplicated it in x direction and replaced one of V atoms by Al atom as shown in Figure (3.4).

The number of k points is chosen to be 64 with 25 k points in the IBZ with 2×5×5 Kmesh of points.

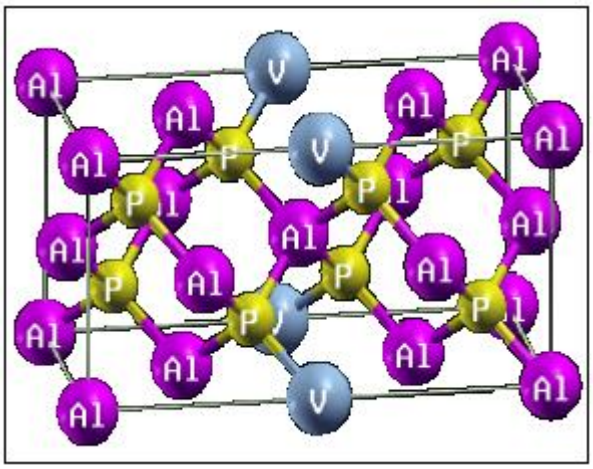

Figure (3.4): Unit cell used to simulate the $Al_{1-x}V_xP$ alloys in ZB structure, x = 0.125.

3.3 Structural properties

In order to know the structural properties (like lattice parameter (a_0), bulk modulus (B_0) and pressure derivative of bulk modulus (B')) for any binary compound, a guess value of lattice constant should be feeded (close to experimental value if it is available) . Then, by fitting the volume versus total energy for binary compounds using Murnaghan's equation (equation 1) of state [50], the structural properties can be determined. This operation is called volume optimization method. Accordingly,

$$E(V) = E_0(V) + \frac{B_0 V}{B'(B'-1)}[B_0(1-\frac{V_0}{V}) + (\frac{V_0}{V})^{B'} - 1. \qquad (3.1)$$

Where E_0 and V_0 are total energy and volume, respectively, at ambient pressure.

For alloys, the operation is the same except that we insert the approximation value of lattice constant with assistance of Vegard's law [51]

$$a_{A_{1-x}B_xC} = (1-x)a_{AC} + (x)a_{BC}, \qquad (3.2)$$

where x is concentration of V, $a_{A_{1-x}B_xC}$ is lattice parameter for the $Al_{1-x}V_xP$ alloy, a_{AC} is lattice parameter for AlP compound and a_{BC} is lattice parameter for VP compound.

3.3.1 Binary compounds: AlP and VP in ZBS

For a binary compound, the volume V of a primitive unit cell in ZB structure for face centred cubic (FCC) is given by

$$V = \frac{1}{4}a_0^3, \qquad (3.3)$$

where a_0 is lattice parameter of the compound.

Making the volume optimization and using equation (3.3), lattice parameter for AlP and VP using LSDA and GGA approximation can be calculated, (1 Bohr = 0.529177 Å).

Using volume optimization curve shown in Figure (3.5a) and equation (3.3), the lattice parameter for AlP is calculated using LSDA and GGA approximations. It was found that, its minimum energy $E_0 = -1165.947615\ (Ry)$ occurs at the volume $V_0 = 271.2068\ (a.u)^3$, and

hence at the lattice constant $a_0 = 5.43$ Å, within LSDA method. Figure (3.5b) and equation (3.3) also used to calculate the minimum energy, $E_0 = -1167.826604\ (Ry)$ occurs at the volume $V_0 = 276.7553\ (a.u)^3$, hence at the lattice constant $a_0 = 5.47$ Å using GGA method. Similarly, the lattice parameter for VP compound is calculated using its volume optimization curves shown in Figure (3.6) and equation (3.3) using LSDA method, Figure (3.6 a) with equation (3.3) show that this compound has a minimum energy $E_0 = -2576.846886\ (Ry)$ at the volume $V_0 = 247.8101\ (a.u)^3$, and hence at the lattice constant $a_0 = 5.27$ Å. Figure (3.5b) and equation (3.3) show that the minimum energy $E_0 = -2582.850035\ (Ry)$ occurs at the volume $V_0 = 258.1041\ (a.u)^3$, and hence at the lattice constant $a_0 = 5.35$ Å using GGA method.

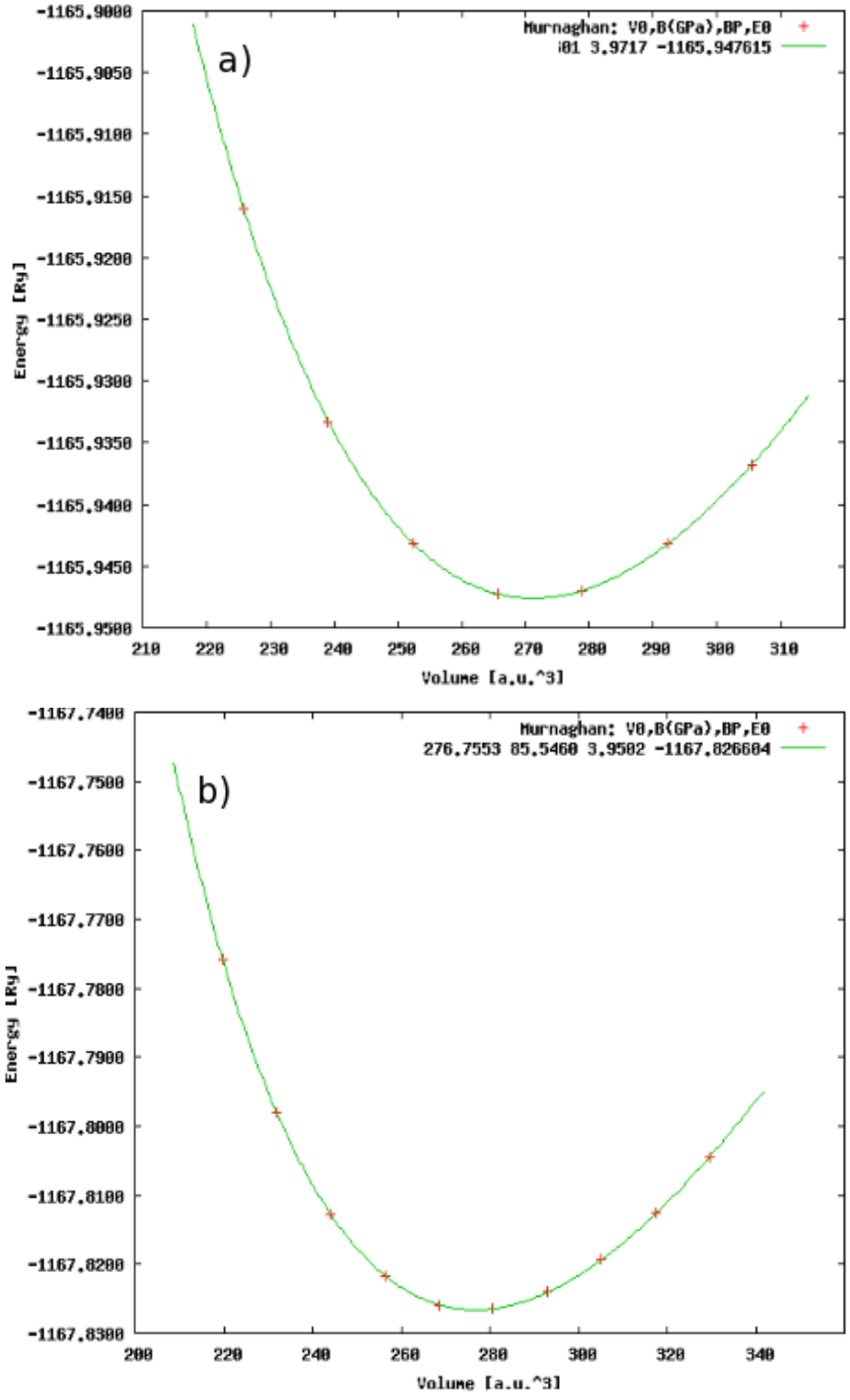

Figure (3.5): Total energy dependence on volume in ZB structure for AlP using: (a) LSDA approximation and (b) GGA approximation.

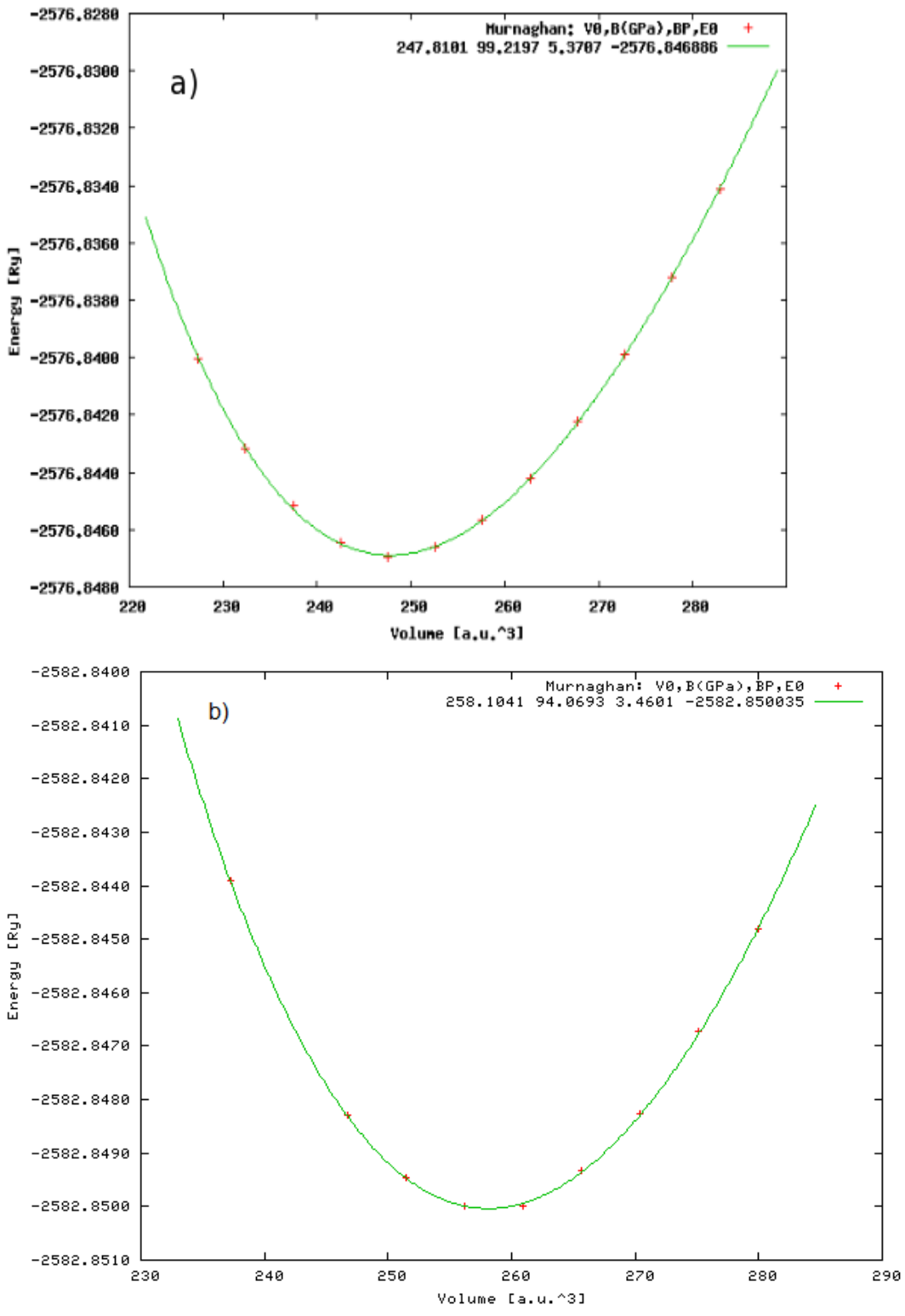

Figure (3.6) :Total energy dependence on volume in ZB structure for VP using : (a) LSDA approximation and (b) GGA approximation.

Calculated results are presented in Table (3.1) for AlP compound, and in Table (3.2) for VP compound. It is worth noting that the value of E_0 using GGA approximation is less than its value using the LSDA approximation. This is an indication that the GGA method is more accurate than LSDA method in calculating E_0 .

For AlP, it is shown that the bulk modulus (B_0) is found to be 89 GPa using LSDA method. By using GGA method, however, B_0 is found to be 85 GPa. For VP, B_0 is found to be 99 GPa using LSDA method, and B_0 equals 94 GPa using GGA method. This means that VP is more hardness than AlP (i. e., VP compound needs more pressure than AlP to change its volume one unit).

The calculations also show that B' for AlP is 4 using both methods, but it is 5 and 3 for VP using LSDA and GGA methods, respectively.

Table (3.1): Equilibrium lattice constant (a_0), bulk modulus (B_0) and pressure derivative of the bulk modulus (B') for AlP compound in the ZB structure using LSDA and GGA approximations.

Method approach	**Lattice constant a_0 (Å)**	**Bulk modulus $B_0(GPa)$**	**Pressure derivative B'**
LSDA (present work)	5.4374	89.3601	3.9717
GGA08 (present work)	5.4742	85.5460	3.9502
Experimental	5.4635^{a}	-	-
Other L(s)DA calculations	$5.43^{b}, 5.44^{c}$ $5.42^{d}, 5.434^{e}$ $5.44^{f}, 5.436^{g}$ $5.462^{h}, 5.417^{i}$ $5.4^{j}, 5.424^{k}$	$90.46^{b}, 90.9^{c}$ $86.5^{d}, 85.5^{e}$ $95.5^{f}, 89^{g}$ 88.6^{i} $90^{j,k}$	$3.72^{b}, 4.24^{c}$ 3.9^{e} 4.14^{g} 4.037^{i} 4.1^{k}
Other GGA calculations	$5.51^{l}, 5.508^{m}$ $5.52^{c}, 5.511^{n}$ 5.511^{g}	$83.23^{l}, 81.52^{m}$ $83.2^{c}, 82.097^{n}$ 82^{g}	$4.02^{l}, 3.89^{m}$ $3.7^{c}, 4.08^{n}$ 3.99^{g}
Other calculations	5.471^{o} 5.421^{p}	84.5^{o} -	4.18^{o} -

a:[1], b:[5], c:[12], d:[15], e:[7], f:[8], g:[13], h:[20], i:[16], j:[18], k:[14], l:[4], m:[11], n:[10], o:[17], p:[19].

It is observed from Tables (3.1) that the present calculations are very close to the theoretical and experimental results. The results of GGA method, however, is closer to experimental results than the results obtained from LSDA approximation, because GGA method take into consideration spin density for both the point itself and it's neighbors which makes it more accurate. It is also worth noting that the values within LSDA method are underestimated, while the values within GGA approximation are overestimated.

Table (3.2): Equilibrium lattice constant (a_0), bulk modulus (B_0) and pressure derivative of the bulk modulus (B') for VP compound in the ZB structure using LSDA and GGA approximations.

Structural parameters	**Present work**		**Experimental**
	LSDA	**GGA**	
Lattice constant a_0 (Å)	5.2763	5.3483	5.27[a]
Bulk modulus $B_0(GPa)$	99.219	94.069	-
Pressure derivative B'	5.3707	3.4601	-

a[24],

It is observed from Tables (3.2) that the present calculations are very close to the experimental results.

3.3.2 $Al_{1-x}V_xP$ alloys at x= 0.125, 0.25, 0.5 and 0.75

The volume of the unit cell of ZB structure for $Al_{1-x}V_xP$ alloy is given by

$V = a^3$ For x=0.25, 0.5 and 0.75 (3.4)

and

$V = 2a^3$ For x= 0.125 (3.5)

Figures (3.7), (3.8), (3.9) and (3.10) present the energy volume optimization for x= 0.125, 0.25, 0.5 and 0.75, respectively. Using Figures (3.8), (3.9), (3.10) along with equation (3.4), the equilibrium lattice constants have been calculated at the minimum total energy point seen in Table (3.3) using LSDA and GGA approximations. For x=0.125, however, the equilibrium lattice constant using LSDA and GGA approximations has been calculated using Figures (3.7) at the minimum total energy point shown in Table (3.3) along with equation (3.5) (the volume of the lattice in this concentration is double the others, because two unit cells were taken in the calculations).

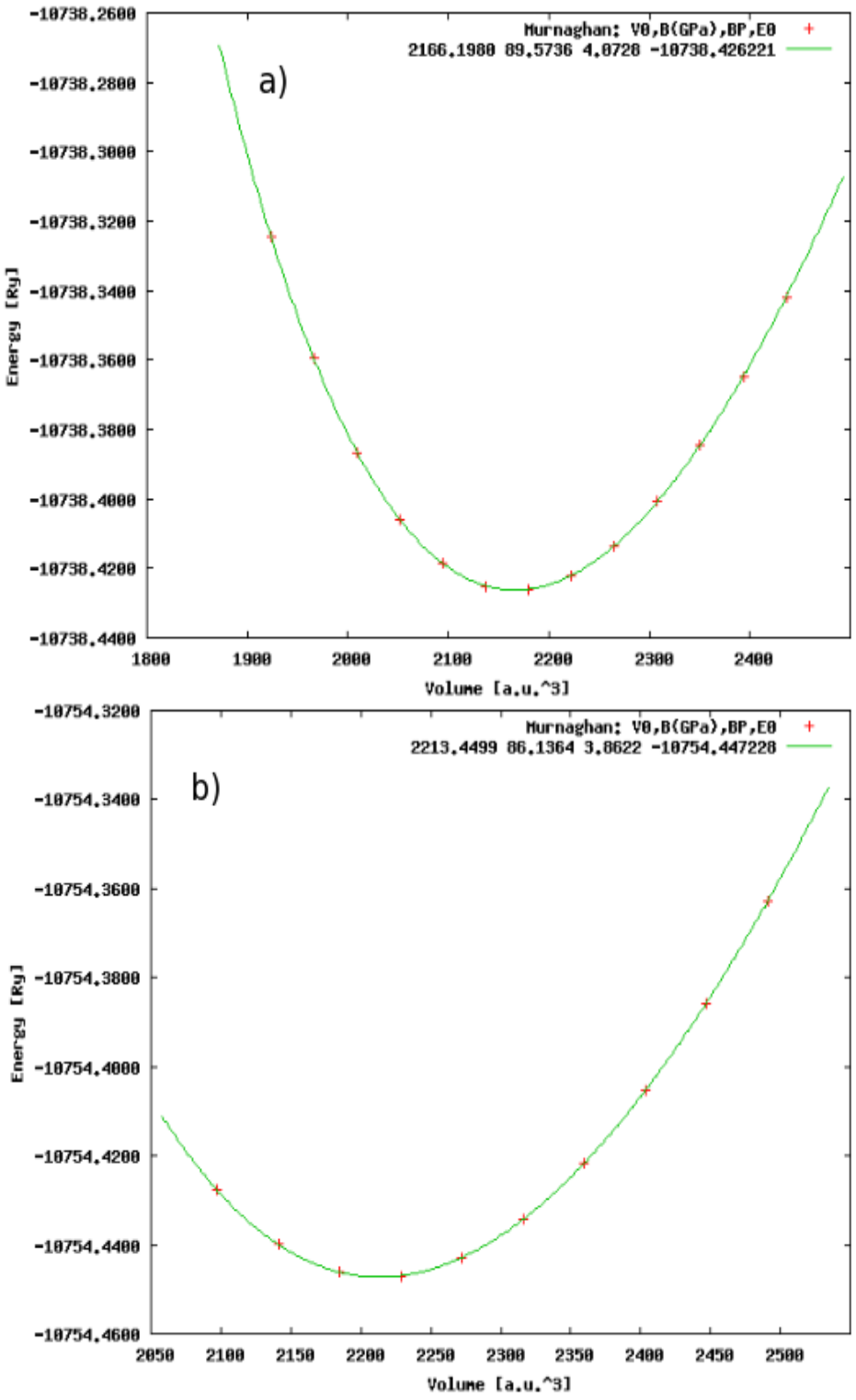

Figure(3.7) :Total energy dependence on volume in ZB structure for $Al_{1-x}V_xP$, x= 0.125 using a) LSDA approximation and (b) GGA approximation.

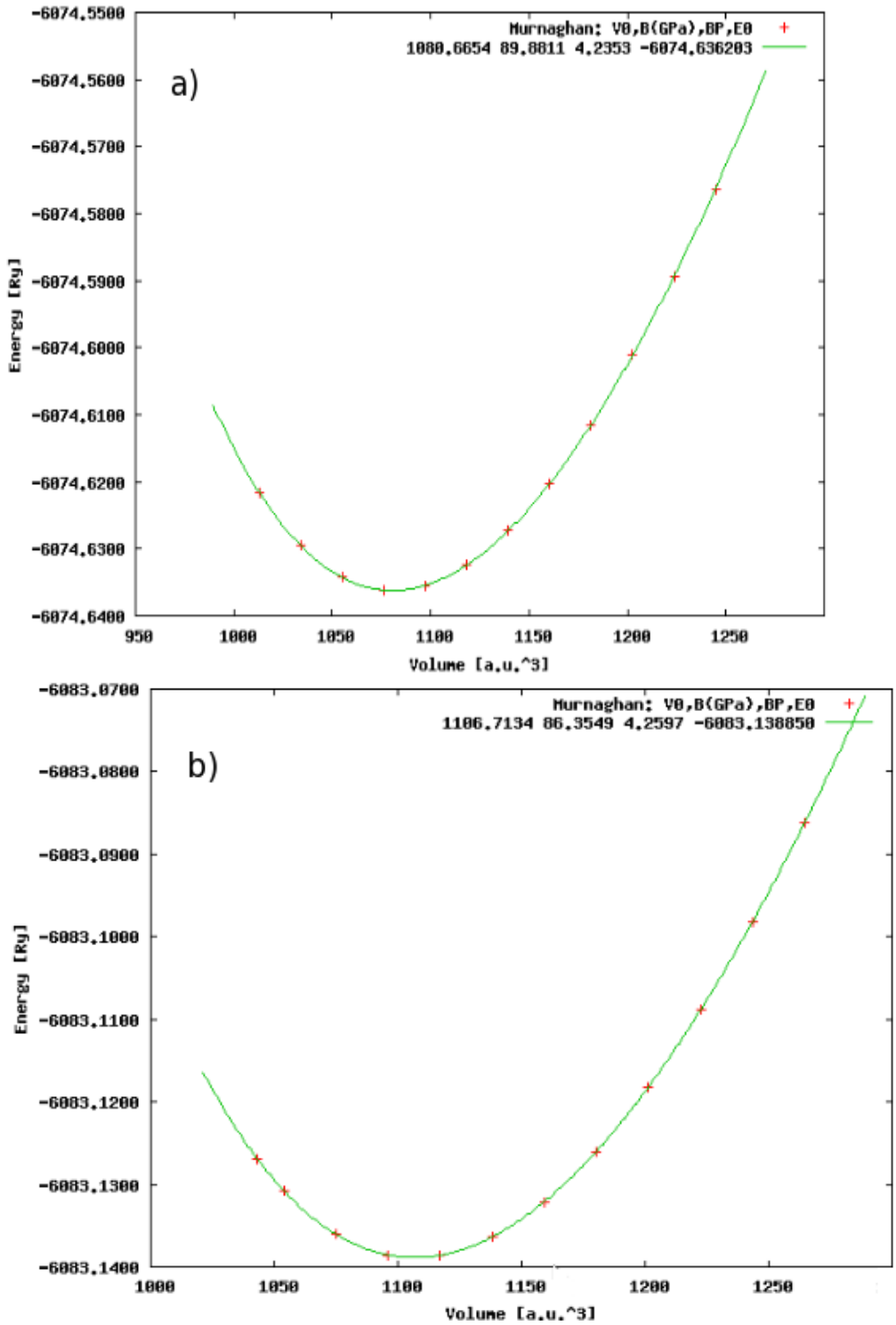

Figure(3.8) : Total energy dependence on volume in ZB structure for $Al_{1-x}V_xP$, x= 0.25 using : (a) LSDA approximation and (b) GGA approximation.

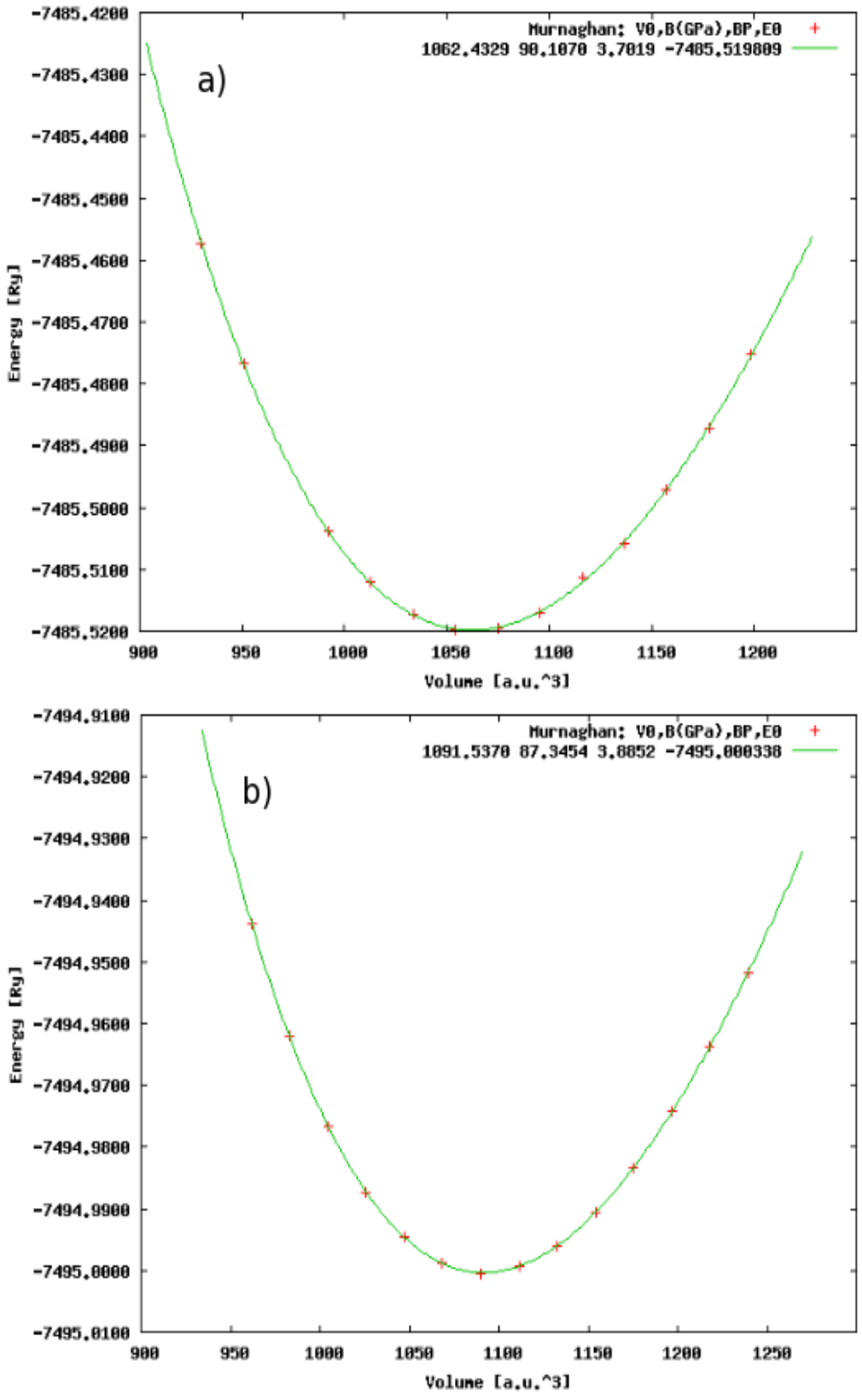

Figure(3.9) : Total energy dependence on volume in ZB structure for $Al_{1-x}V_xP$, x= 0.5 using : (a) LSDA approximation and (b) GGA approximation.

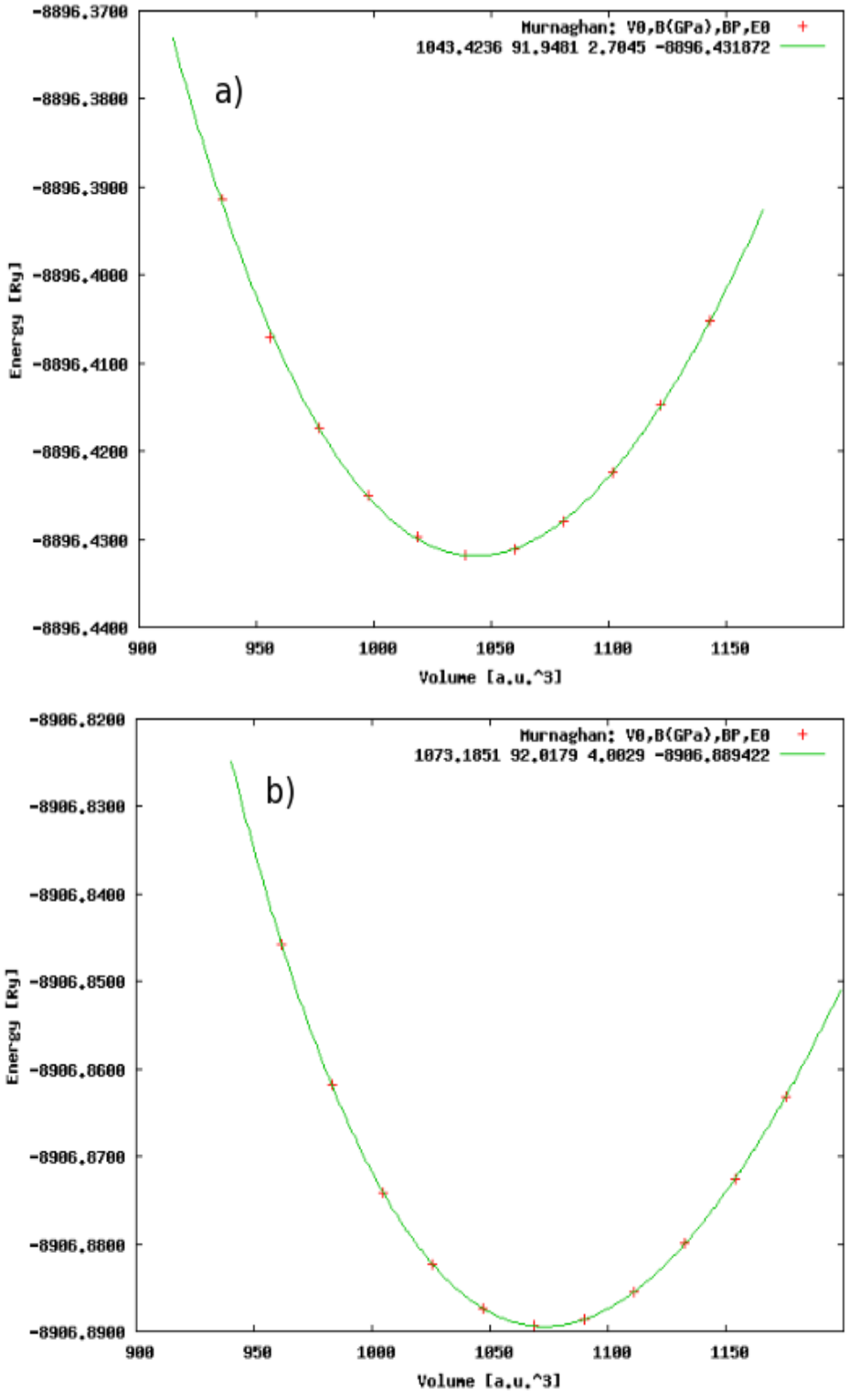

Fig(3.10) : Total energy dependence on volume in ZB structure for $Al_{1-x}V_xP$, x= 0.75 using : (a) LSDA approximation and (b) GGA approximation.

The minimum total energy E_0 using GGA method is less than that of LSDA method for each concentration, as illustrated in Table (3.3).

Table (3.3) : Total minimum energy (E_0) in Rydberg (Ry) for $Al_{1-x}V_xP$ alloys with concentration (x= 0.125, 0.25, 0.5 and 0.75) in ZB structure using LSDA and GGA approximations.

Concentration	**Minimum total energy E_0 (Ry)**	
	LSDA	**GGA**
0.125	-5369.213110	-5377.223614
0.25	-6074.636203	-6083.138850
0.5	-7405.519809	-7495.000338
0.75	-8896.431872	-8906.889422

Table (3.3) illustrate that the total minimum energy decreases as the concentration of vanadium increases, because the vanadium has a strong magnetic and it makes the alloy ferromagnetic which has lower energy.

The calculated equilibrium lattice constants for various concentrations using LSDA and GGA approximations are summarized in Table (3.4). Additionally, the calculated values of bulk modulus B_0 and its derivative B' using LSDA and GGA approximations for $Al_{1-x}V_xP$ when x=0.125, 0.25, 0.5 and 0.75 have been presented in Table (3.4).

Table (3.4) : The structural properties of $Al_{1-x}V_xP$ alloys (x=0.125, 0.25, 0.5 and 0.75) in ZB structure using LSDA and GGA approximations.

	Method approach (present work)	**Lattice constant a_0 (Å)**	**Bulk modulus $B_0(GPa)$**	**Pressure derivative B'**
$Al_{1-x}V_xP$ **x=0.125**	**LSDA**	5.4338	89.5736	4.0728
	GGA08	5.47369	86.1364	3.8622
$Al_{1-x}V_xP$ **x=0.25**	**LSDA**	5.4304	89.8811	4.2353
	GGA08	5.47367	86.3549	4.2597
$Al_{1-x}V_xP$ **x=0.5**	**LSDA**	5.3997	90.1070	3.7019
	GGA08	5.4485	87.3454	3.8852
$Al_{1-x}V_xP$ **x=0.75**	**LSDA**	5.3673	91.9481	2.7045
	GGA08	5.4178	92.0179	4.0029

From Table (3.4), it can be concluded that the radius of vanadium is smaller than that of aluminium. It was a matter of disagreement between some of the researchers, some of them see that vanadium radius is larger than that of aluminium [52] , others see the opposite [53].

Figure (3.11) below describes the relation between the concentration of vanadium V and lattice parameter (a_0) using LSDA and GGA

approximations.

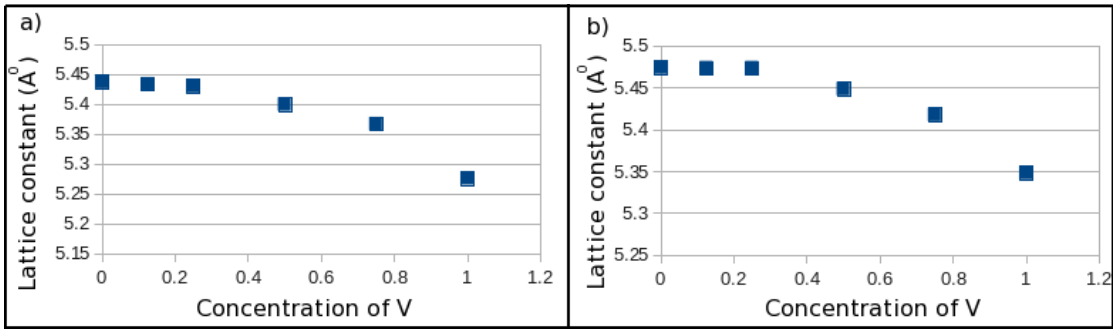

Figure (3.11): lattice constant variation with V concentration for $Al_{1-x}V_xP$ using: (a) LSDA method and (b) GGA method.

In Figure (3.11), it is shown that the lattice constant of the compound decreases as the concentration of vanadium increases. This observation leads to the conclusion that the radius of vanadium is smaller than aluminum as mentioned previously.

Figure (3.12) shows the relation between concentration of V and the bulk modulus B_0 using LSDA and GGA approximations.

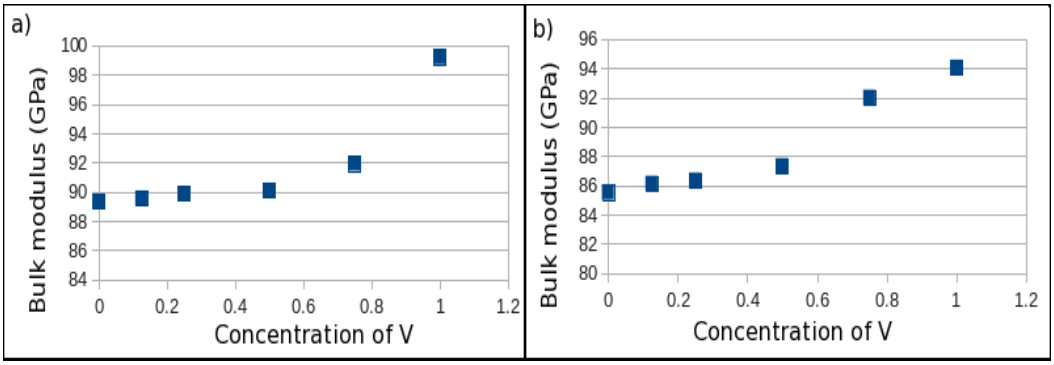

Figure (3.12): Bulk modulus variation with V concentration for $Al_{1-x}V_xP$ using:(a) LSDA method and (b) GGA method.

Figure (3.12) indicates that the bulk modulus B_0 increases as concentration of V increases. This means that the alloy of interest becomes harder as the concentration of vanadium increases.

To know which of LSDA and GGA is more accurate, the percentage errors in these calculations versus experimental results for AlP and VP compound have been presented in Table (3.5). Table (3.5) shows that the GGA approximation is more precise than LSDA approximation for AlP . In contrast the GGA approximation is less precise than LSDA approximation for VP because NiAs structure is not considered as the ground state for VP, instead of that ZB structure is considered.

Table(3.5): The percentage errors in AlP and VP for a_0 using LSDA and GGA approximations.

Compound	LSDA	GGA
	a_0	a_0
AlP	0.48%	0.19%
VP (ZB)	0.1%	1.5%

3.4 Electronic properties

In free atoms at 0 Kelvin (K), electrons are arranged in discrete energy levels. When a huge number of atoms gather together and interact with each other to form a crystalline solid, the adjacent energy states (i. e., energy bands) will replace previous discrete energy states. The highest filled energy band of electrons is called valence band, the lowest unfilled

energy band is called conduction band. The distance between the top of valence band and the minimum of conduction band is called the energy gap. If the top of valence band and minimum of conduction band are at the same symmetry line in BZ, then the energy band gap is called direct energy band gap. Otherwise it is called indirect energy band gap.

From the value of energy band gap we can specify if the solid is insulator, semiconductor, semi-metal or metal. Using WIEN2K-code and plotting band structure graphs, we will clarify those types of the solid as shown in the next sections.

3.4.1 Binary compounds: AlP and VP in ZB structure

Figure (3.13) illustrated the band structure for AlP in ZB structure using LSDA and GGA approximations, respectively. These figures show that the Fermi energy E_f is on the top of valence band along the Γ symmetry line; while the minimum of conduction band is along X symmetry line. The difference between top of valence band and minimum of conduction band is about 1.43 eV and 1.63 eV, respectively, using LSDA and GGA methods. This implies that the AlP compound is a semiconductor material with indirect band gap energy. It is worth noting that the energy band gap for GGA is larger than LSDA because of the difference in their lattice parameters.

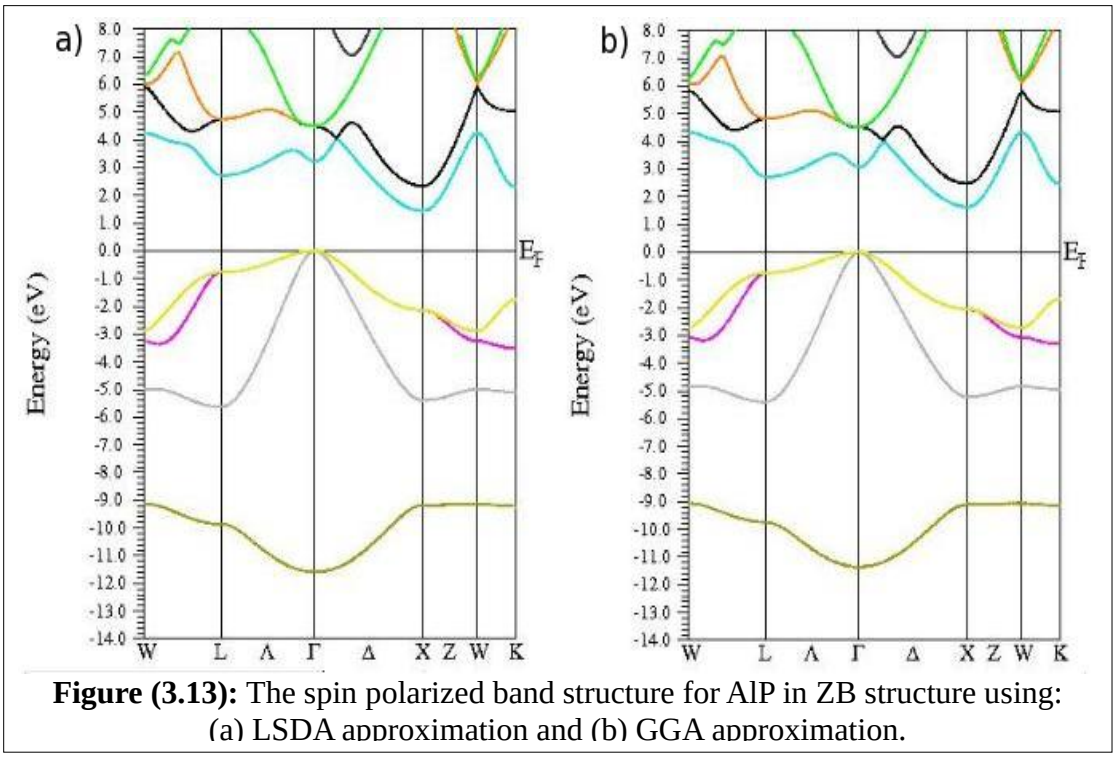

Figure (3.13): The spin polarized band structure for AlP in ZB structure using: (a) LSDA approximation and (b) GGA approximation.

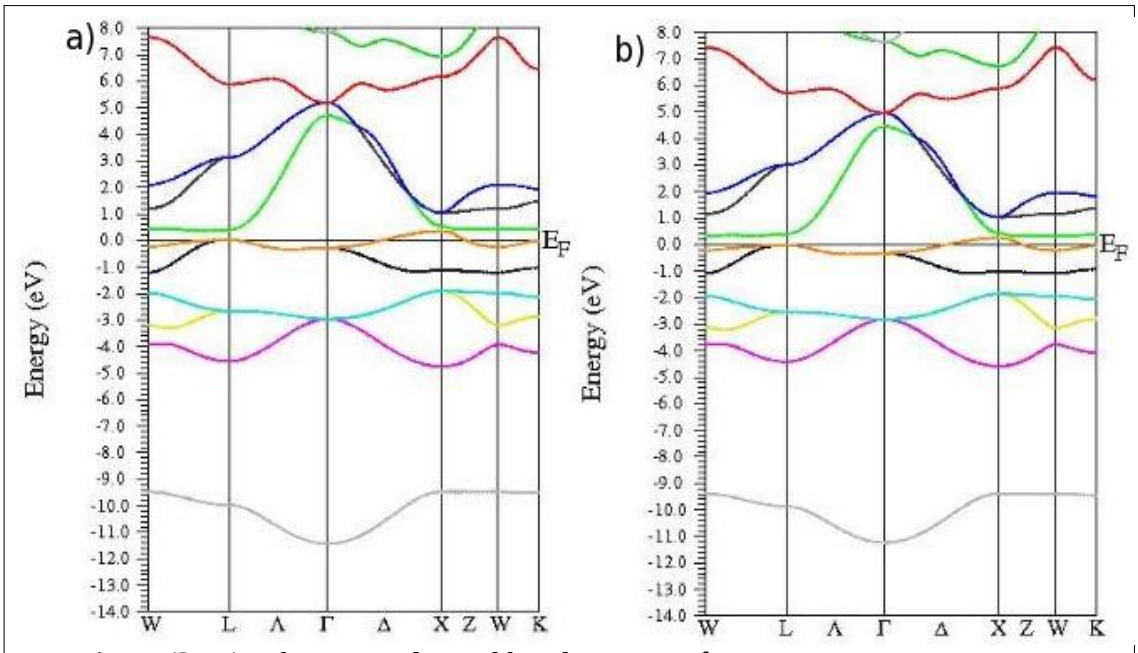

Figure(3.14): The spin polarized band structure for VP in ZB structure using: (a) LSDA approximation and (b) GGA approximation.

Similarly, Figure (3.14) illustrates the band structure for VP in ZB structure using LSDA and GGA approximations, respectively. From these figures, it is clearly seen that the Fermi energy crosses the valence and conduction bands due to the hybridization between V-d state with P -p state. This indicates that the VP compound is a metal.

Table (3.6) summarizes our results as well as other theoretical and experimental results of the energy band gap for AlP. This table shows that the GGA result is closer to experimental value than LSDA method. The percentage error in energy gap of AlP is 42% for LSDA approximation and 34% for GGA approximation, which makes GGA approximation more precise than LSDA approximation in calculating the energy band gap.

Table (3.6): The Calculated and The experimental energy band gap (E_g) in eV for AlP in ZB structure using LSDA and GGA approximations.

Compound	Method approach	Energy gap E(eV)
AlP	**LSDA (present)**	1.43821
	GGA08 (present)	1.63845
	Experimental results	2.505[a]
	Other LDA calculations	1.41[b] ,1.49[c] 1.44[d] ,2.17[e]
	Other GGA calculations	1.635[f] ,2.49[g] 1.632[h] ,1.57[d]

a:[3], b:[5], c:[9], d:[13], e:[20], f:[11], g:[12] ,h:[10].

3.4.2 $Al_{1-x}V_xP$ alloys at x= 0.125, 0.25, 0.5 and 0.75

Figures (3.15), (3.16), (3.17) and (3.18) present the band structure for $Al_{1-x}V_xP$ in ZB structure using LSDA and GGA approximations for x= 0.125, 0.25, 0.5 and 0.75, respectively. Figure (3.15) shows that the conduction and valence bands almost overlap with others. The zero energy band gap using LSDA method; whereas the energy band gap using GGA method is very small (0.3 eV). In contrast, Figures (3.16), (3.17) and (3.18) indicate that the conduction and valence bands overlap with zero energy gap. Hence, $Al_{1-x}V_xP$ in ZB structure is a metal for x=0.25, 0.5 and 0.75 concentrations. This implies that the band gap energy of $Al_{1-x}V_xP$ is strongly effected by vanadium because vanadium is a strong metal.

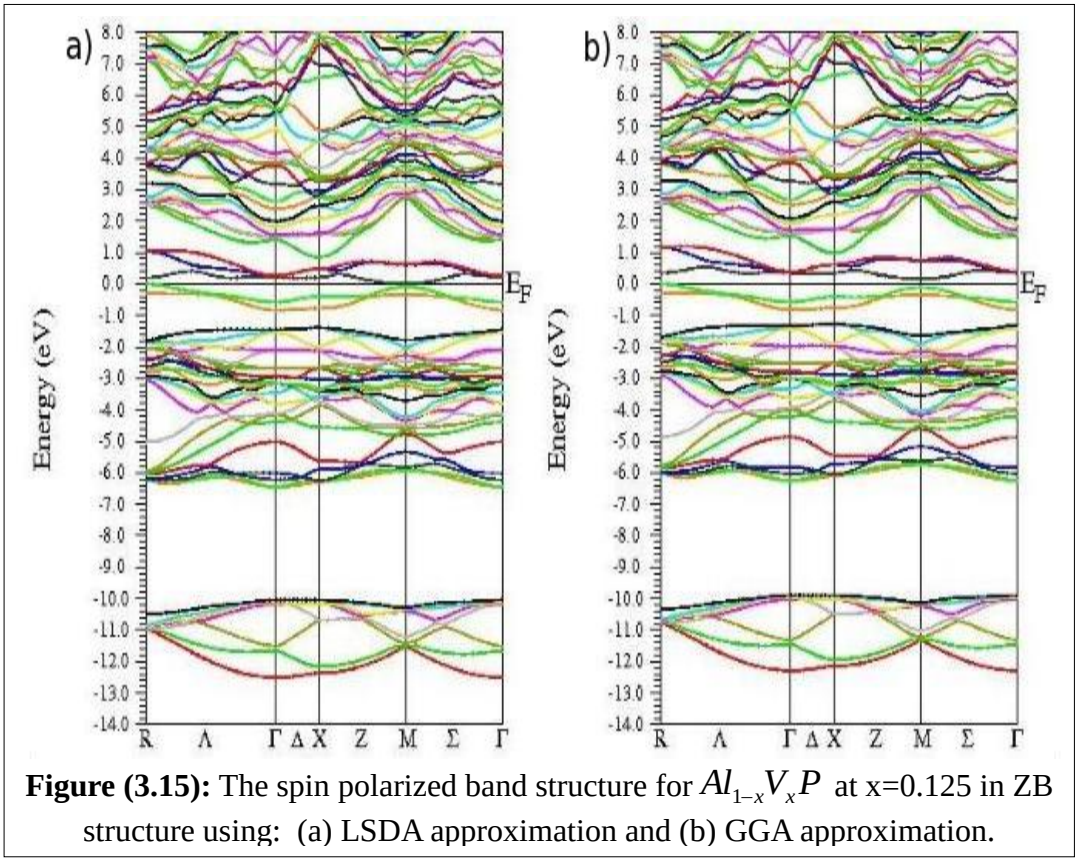

Figure (3.15): The spin polarized band structure for $Al_{1-x}V_xP$ at x=0.125 in ZB structure using: (a) LSDA approximation and (b) GGA approximation.

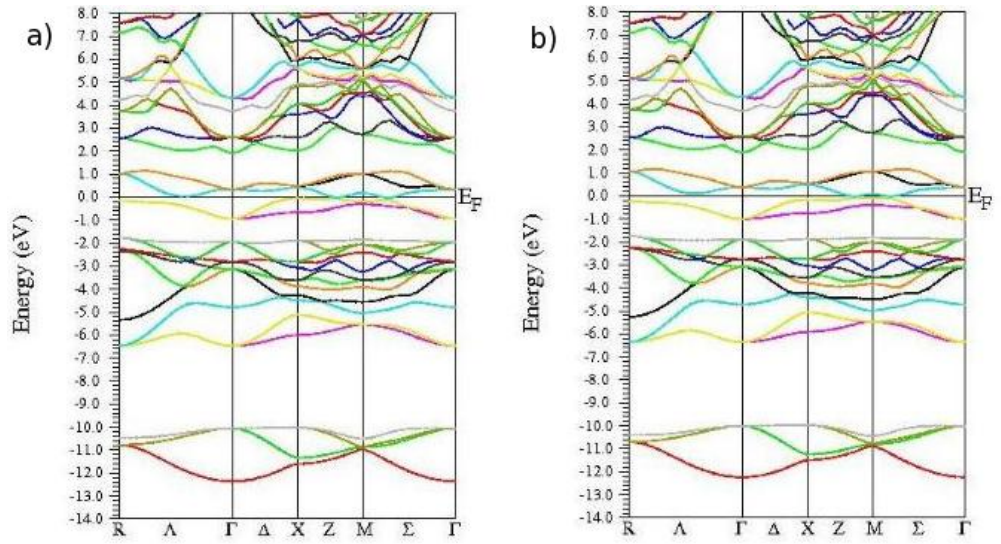

Figure (3.16) : The spin polarized band structure for $Al_{1-x}V_xP$, x=0.25 in ZB structure using: (a) LSDA approximation and (b) GGA approximation.

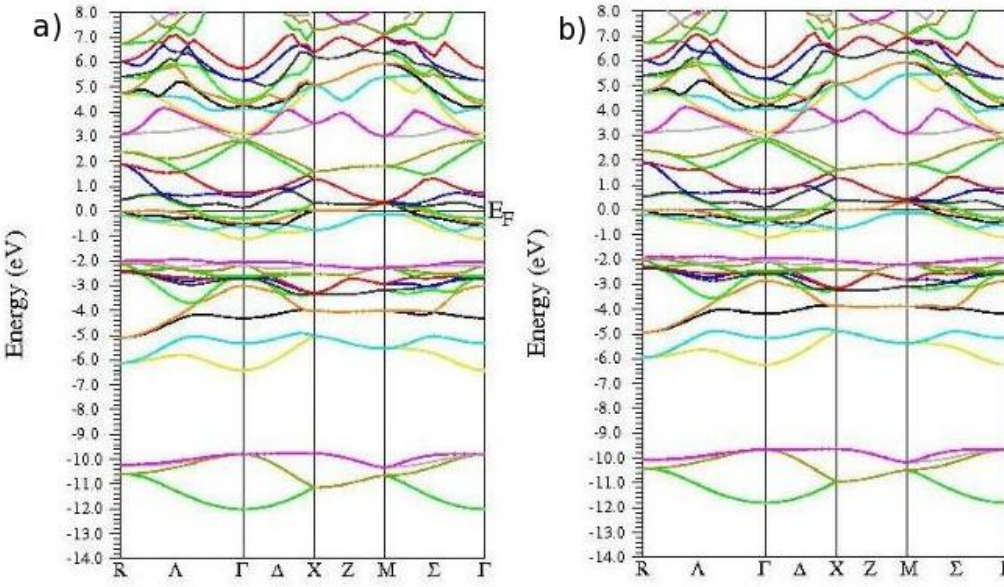

Figure (3.17) : The spin polarized band structure for $Al_{1-x}V_xP$, x=0.5 in ZB structure using: (a) LSDA approximation and (b) GGA approximation.

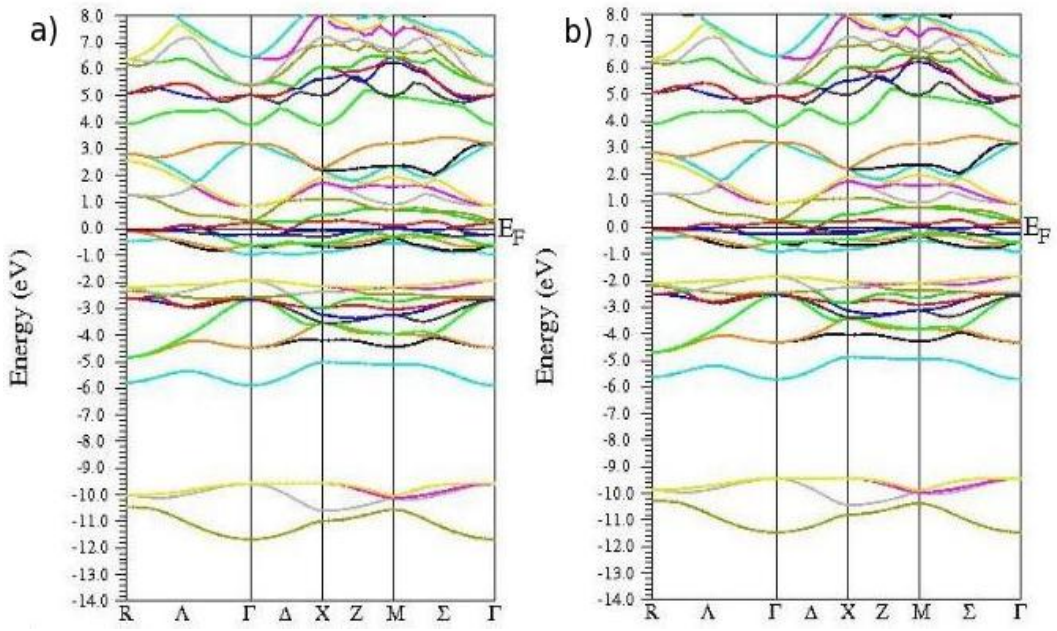

Figure (3.18) : The spin polarized band structure for $Al_{1-x}V_xP$, x=0.75 in ZB structure using: (a) LSDA approximation and (b) GGA approximation.

Table (3.7) summarizes the energy band gap for $Al_{1-x}V_xP$ alloy for x=0.125. For $Al_{1-x}V_xP$ alloys, it can be concluded that the energy gap decreases as the concentration of the vanadium increases. Therefore, $Al_{1-x}V_xP$ were semiconductors for x=0 and 0.125; whereas they were metals for x= 0.25, 0.5, 0.75 and 1.

Table (3.7): The Calculated energy band gap (E_g) in eV for $Al_{1-x}V_xP$ in ZB structure for x=0.125 using LSDA and GGA approximations.

Compound	Method approach	Energy gap E(eV)
$Al_{1-x}V_xP$ (x=0.125)	**LSDA**	0
	GGA	0.3

3.5 Magnetic properties

The total magnetic dipole moment (μ_{tot}) for any system comes from the magnetic moment of the interstitial region as well as the atoms of compounds or alloys. From the total magnetic moment, we can justify whether the compound is diamagnetic, paramagnetic, ferromagnetic or antiferromagnetic.

The present LSDA calculations show that the total magnetic moment per unit cell (μ_{tot}/unit cell) for $Al_{1-x}V_xP$ is almost zero for x=0; whereas it is 2.06382 μ_B, 1.99685 μ_B, 3.99425 μ_B, 5.98478 μ_B, and 1.49720 μ_B for x=0.125, 0.25, 0.5,0.75 and 1, respectively, as shown in Table (3.8). Similarly, the present GGA calculations show that the value of μ_{tot}/unit cell for $Al_{1-x}V_xP$ is almost zero for x=0; whereas it is 2.01317 μ_B, 2.00069 μ_B, 3.99753 μ_B, 6.00272 μ_B, and 1.64528 μ_B for x=0.125, 0.25, 0.5,0.75 and 1, respectively, as shown in Table (3.8). From this table, it is shown that the GGA approximation gives larger values for μ_{tot} than LSDA

approximation, and the results differ by 0.01- $0.025\,\mu_B$. This small difference may be due to the difference in the lattice parameters values.

Table (3.8): Total and local Magnetic Moments for $Al_{1-x}V_xP$ system in ZB structure using LSDA and GGA approximations.

Compound	Magnetic moment (μ)	LSDA (μ_B)	GGA (μ_B)
AlP	interstitial	- 0.01660	- 0.00357
	Al	- 0.00734	- 0.00069
	P	0.00494	0.00133
	μ_{tot} /unit cell	- 0.01899	- 0.00293
$Al_{1-x}V_xP$ x=0.125	interstitial	0.24284	0.21904
	Al	0.03990	0.03467
	V	0.78981	0.81089
	P	- 0.04065	- 0.05802
	μ_{tot} /unit cell	1.03191	1.00658
$Al_{1-x}V_xP$ x=0.25	interstitial	0.44892	0.43096
	Al	0.06507	0.06150
	V	1.57961	1.60179
	P	- 0.09676	- 0.09356
	μ_{tot} /unit cell	1.99685	2.00069

$Al_{1-x}V_xP$ x=0.5	interstitial	0.92154	0.89290
	Al	0.06820	0.06254
	V	3.16176	3.27134
	P	- 0.15724	- 0.22924
	μ_{tot} /unit cell	3.99425	3.99753
$Al_{1-x}V_xP$ x=0.75	interstitial	1.31949	1.30050
	Al	0.04137	0.03637
	V	4.83993	4.99734
	P	- 0.21600	- 0.33152
	μ_{tot} /unit cell	5.98478	6.00272
VP	interstitial	0.26006	0.29556
	V	1.27888	1.42596
	P	- 0.04174	- 0.07624
	μ_{tot} /unit cell	1.49720	1.64528

From Table (3.8) as well as from Figure (3.19), it can be seen that the largest contribution in the total magnetic moment comes from V atoms. Their contributions using LSDA and GGA approximations, respectively, are 76.5% and 80.5% for x=0.125, 79.1% and 80% for x=0.25, 79.15% and 81.8% for x=0.5, 80.8% and 83.3% for x=0.75 and 85.4% and 86.7% for x=1. Although there is a little contribution by Al atoms and interstitial region, there is a loss in the total magnetic moment by P atoms. This leads

us to conclude that the main contribution for total magnetic moment is due to V atoms.

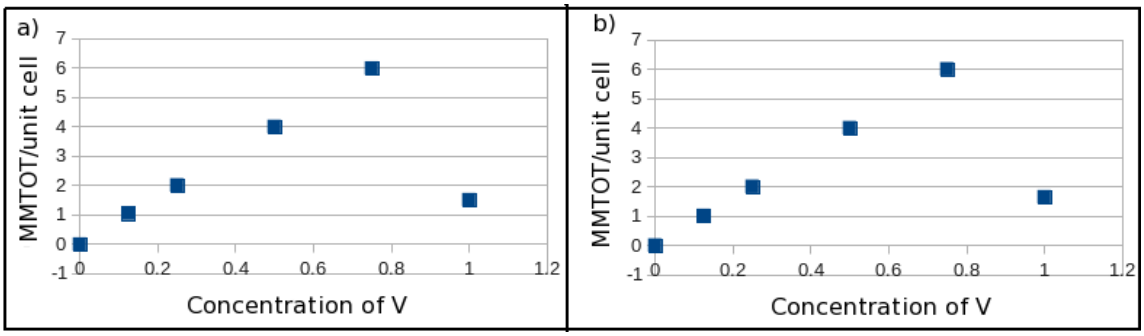

Figure (3.19): The relation between concentration of V and total magnetic moment (μ_{tot})/unit cell using:(a) LSDA approximation and (b) GGA approximation.

In addition, Table (3.8) as well as Figure (3.19) show that the μ_{tot} increases as the concentration of V increases with the existence of Al. This indicates that the most important role in determining the value of μ_{tot} for the system of interest is due to the concentration of V atoms in the presence of Al atoms. In other words, V-V spin interactions and V-Al spin interactions play a critical role in determining the value of μ_{tot}. Therefore, μ_{tot} decreases for x=1, because the V-Al spin interactions vanish in this case.

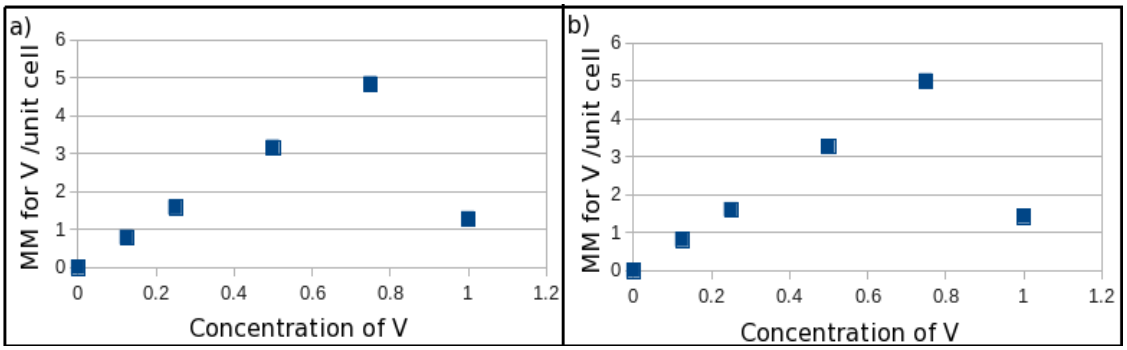

Figure (3.20): The relation between concentration of V and the magnetic moment (μ) for V atom /unit cell using: (a) LSDA approximation and (b) GGA approximation.

Figure (3.20) show that the μ of V per unit cell increases as the concentration of V increases.

3) The equilibrium lattice parameter, energy band gap and μ_{tot} for every concentration using GGA method are larger than LSDA method, whereas the bulk modulus using GGA method is smaller than that of LSDA method.

4) The present calculated results using GGA method is more accurate than LSDA method because

a) the total energy of equilibrium lattice parameter using GGA method is smaller than that of LSDA method.

b) the calculated lattice constant, Bulk modulus and energy band gap for AlP compound using GGA method are closer to the experimental values than that of LSDA method.

5) The energy band gap is dependent on the concentration of doped V; While the concentration of V increases, the energy band gap decreases and it is vanishes after x=0.125.

6) The doped V transforms AlP compound in ZB structure from semiconductor to metal.

7) The total magnetic moment μ_{tot} is dependent on the concentration of doped V. While the concentration of V increases, the lattice parameter increases as the concentration of V increases.

Future work:

For future work, I would like to carry on more research on the AlP compound and calculate its other physical properties such as density of states and transition pressure, for different structures.

References

[1] Nelmes, R.J. and McMahon M.I. **Semiconductors and semimetals**. London: Academic Press; 1998. Vol. 54. p.185.

[2] Greene R.G., Luo H. and Ruoff A.L. 1994. **High pressure study of AlP: Transformation to a metallic NiAs phase**. J. Appl. Phys. 76 (11): 7296-7299.

[3] Monemar B. 1973. **Fundamental Energy Gaps of AlAs and Alp from Photoluminescence Excitation Spectra**. Phys. Rev. B. 8 (12): 5711-5718.

[4] Arbouche O., Belgoumene B., Soudini B., Azzaz Y., Bendaoud H. and Amara K. 2010. **First-principles study on structural properties and phase stability of III-phosphide (BP, GaP, AlP and InP).** Computational Materials Science 47: 685-692.

[5] Aouadi S., Rodriguez-Hernandez P., Kassali K. and Muñoz A. 2008. **Lattice dynamics properties of zinc-blende and Nickel arsenide phases of AlP.** Physics Letters A 372: 5340-5345.

[6] Razeghi, M. Thin films: **Heteroepitaxial systems**. London: World Scientific; 1999. Vol. 15. p 460.

[7] Saeed Y., Shaukat A., Nazir S., Ikram N. and Reshak A.H. 2010. **First principles calculations of electronic structure and magnetic**

properties of Cr-based magnetic semiconductors $Al_{1-x}Cr_xX$ **(X=N, P, As, Sb)**. Journal of Solid State Chemistry 183: 242-249.

[8] Kulkova S.E., Khanin D.V. and Subashiev A.V. 2005. **Simulation of Na, K, Cs and Cs(O) adsorption on GaAs(110) and (100) surfaces: towards predictable electronic structure of activation layer**. Nuclear Instruments and Methods in Physics Research A 536: 295-301.

[9] Reshak A.H. and Auluk S. 2007. **Investigation of the electronic properties, first and second harmonic generation for** $A^{XIII}B^{XV}$ **zinc-blende semiconductors**. Physica B 395: 143-150.

[10] Annane F., Meradji H., Ghemid S. and El Haj Hassan F. 2010. **First principle investigation of AlAs and AlP compounds and ordered** $AlAs_{1-x}P_x$ **alloys**. Computational Materials Science 50: 274-278.

[11] Yu L.H., Yao K.L. and Liu Z.L. 2005. **Electronic band structures of filled tetrahedral semiconductor LiMgP and zinc-blende AlP. Solid State Communications** 135: 124-128.

[12] Briki M., Abdelouhab M., Zaoui A. and Ferhat M. 2009. **Relativistic effects on the structural and transport properties of III-V compounds: A first-principles study**. Superlattices and Microstructures 45: 80-90.

[13] Ahmed R., Aleem F.e., Hashemifar S.J. and Akbarzadeh H. 2008. **First-principles study of the structural and electronic properties of III-**

phosphides. Physica B 403: 1876-1881.

[14] Mujica A., Rodríguez-Hernández P., Radescu S., Needs R.J. and Muñoz A. 1999. **AlX (X = As, P, Sb) Compounds under Pressure**. Phys. Stat. Sol. (b) 211: 39-43.

[15] Froyen S. and Cohen M.L. 1983. **Structural properties of III-V zinc-blende semiconductors under pressure**. Physical Review B 28 (6): 3258-3265.

[16] Wang S.Q. and Ye H.Q. 2002. **Plane-wave pseudopotential study on mechanical and electronic properties for IV and III-V crystalline phases with zinc-blende structure**. Physical Review B 66 (23):23511-1-7.

[17] Zhang S.B. and Cohen M.L. 1987. **High-pressure phases of III-V zinc-blende semiconductors**. Physical Review B 35 (14): 7604-7610.

[18] Rodríguez-Hernández P. and Muñoz A. 1992. **Ab initio calculations of electronic structure and elastic constant in AlP**. Semicond. Sci. Technol. 7: 1437-1440.

[19] Yeh C.Y., Lu Z. W., Froyen S. and Zunger A. 1992. **Zinc-blende wurtzite polytypism in semiconductors**. Physical Review B 46 (16): 10086-10097.

[20] Huang M.Z. and Ching W.Y. 1993. **Calculation of optical excitations in cubic semiconductors. I. Electronic structure and linear**

response. Physical Review B 47 (15): 9449-9463.

[21] Kornilov I.I. and Matveeva N.M. 1962. **The metal chemistry of Vanadium**. Russian Chemical Review 31 (9): 512-520.

[22] Boudin S., Guesdon A., Leclaire A. and Borel M.-M. 2000. **Review on Vanadium Phosphates with mono and divalent metallic cations: syntheses, structural relationships and classification, properties.** International Journal of Inorganic Materials 2: 561-579.

[23] Kematick R.J. and Myers C. E. 1992. **Band Structures of and Bonding in 10-Electron Solids: MnAl, CrSi, VP, TiS**. Inorg. Chem. 31: 3568-3572.

[24] Galanakis I. and Mavropoulos P. 2003. **Zinc-blende compounds of transition elements with N, P, As, Sb, S, Se, and Te as half-metallic systems**. Physical Review B 67: 104417-1-8.

[25] MacDonald A.H., Schiffer P. and Samarth N. 2005. **Ferromagnetic semiconductors: moving beyond (Ga,Mn)As.** Nature Materials 4: 195-202.

[26] Wolf S.A., Awschalom D.D., Buhrman R.A., Daughton J.M., Molnar S. V., Roukes M.L., Chtchelkanova A.Y. and Treger D.M. 2001. **Spintronics: a spin-based electronics vision for the future**. Science 294: 1488-1495.

[27] Coey J. M. D. Curr, Opin. **Solid State Mater**. Sci. 10 (2): 83-92.

[28] Yang Y., Zhao Q., Zhang X.Z., Liu Z.G., Zou C.X., Shen B. and Yu D.P. 2007. **Mn-doped AlN nanowires with room temperature ferromagnetic ordering.** Applied Physics Letters 90 (9): 092118-1-3.

[29] Reed M.L., El-Masry N.A., Stadelmaier H.H., Ritums M.K. and Reed M.J. 2001. **Room temperature ferromagnetic properties of (Ga, Mn)N**. Applied Physics Letters 79 (21): 3473-3475.

[30] Yang S.G., Pakhomov A.B., Hung S.T. and Wong C.Y. 2002. **Room-temperature magnetism in Cr-doped AlN semiconductor films**. Applied Physics Letters 81 (13): 2418-2420.

[31] Wu S.Y., Liu H.X., Gu L., Singh R.K., Budd L., Schilfgaarde M.V., McCartney M.R., Smith D.J. and Newman N. 2003. **Synthesis, characterization, and modeling of high quality ferromagnetic Cr-doped AlN thin films**. Applied Physics Letters 82 (18): 3047-3049.

[32] Blaha, P. Schwarz, K., Madsen, G. K. H. Kvasnicka D. and Luitz J. **Wien2k, An Augmented Plane Wave + Local Orbitals Program for Calculating Crystal Properties**. Karlheinz Schwarz, Techn. Universitat Wien: Austria; 2001.

[33] Cottenier, S. ***Density Functional Theory and the Family of (L)APW-methods: a step-by-step introduction. Instituut voor Kern-en***

Stralingsfysica, *K.U.Leuven: Belgium; 2002*.

[34] Szabo A and Ostlund N.S. ***Modern Quantum Chemistry***. New York: McGraw-Hill, Inc. 1989. p 53.

[35] Hohenberg P. and Kohn W. 1964. **Inhomogeneous Electron Gas**. Physical Review 136 (3B): B 864- B 871.

[36] Kohn W. and Sham L.J. 1965. **Self-Consistent Equations Including Exchange and Correlation Effects**. Physical Review 140 (4A): A 1133- A 1138.

[37] Payne M.C., Teter M.P., Allan D.C., Arias T.A. and Joannopoulos J.D. 1992. **Iterative minimization techniques for ab initio total-energy calculations: molecular dynamics and conjugate gradients**. Reviews of Modern Physics 64 (4): 1045-1055.

[38] Wood B., Hine N.D.M., **Foulkes W.M.C. and García- González P. 2007. Quantum Monte Carlo calculations of the surface energy of an electron gas**. Physical Review B 76: 035403-1-6.

[39] Vosko S.H. and Wilk L. 1980. **Influence of an improved local-spin-density correlation-energy functional on the cohesive energy of alkali metals**. Physical Review B 22 (8): 3812-3815.

[40] Perdew J.P., Ruzsinszky A., Csonka G.I., Vydrov O.A., Scuseria G.E., Constantin L.A., Zhou X. and Burke K. 2008. **Restoring the Density-**

Gradient Expansion for Exchange in Solids and Surfaces. Physical Review Letters 100 (13): 136406-1-4.

[41] Blügel S. and Bihlmayer G. **Full-Potential Linearized Augmented Planewave Method, John von Neumann Institute for computing**: Jülich; 2006. Vol. 31. p 85.

[42] Slater J.C. 1937. **Wave Functions in a Periodic Potential**. Physical Review 51 (10): 846-851.

[43] Slater J.C. 1964. **Energy band calculations by the augmented plane wave method**. Advances in Quantum Chemistry 1: 35-58.

[44] Anderson O.K. 1975. **Linear methods in band theory**. Physical Review B 12: 3060.

[45] Singh D. 1991. **Ground-state properties of Lanthanum: Treatment of extended-core states.** Physical Review B 43 (8): 6388-6392.

[46] Sjöstedt E., Nordström L. and Singh D.J. 2000. **An alternative way of linearizing the augmented plane wave method**. Solid State Communications 114: 15-20.

[47] Madsen G.K.H., Blaha P., Schwarz K., Sjostedt E. and Nordstrom L. Physical Review B 64 :195134-1-9.

[48] Monkhorst H.J. and Pack J.D. (1976). **Special points for Brillouin-**

Chapter 4
Conclusions and future work

In this study, FP-LAPW method was employed using LSDA and GGA approximations for calculating the structural, electronic and magnetic properties of binary compounds AlP, VP and ternary alloys $Al_{1-x}V_xP$ for x= 0.125, 0.25, 0.5 and 0.75.

Results achieved in this study are in good agreement with experimental and other LSDA and GGA theoretical values for x=0 and 1. To the best of our knowledge, other concentrations (x=0.125, 0.25, 0.5 and 0.75) have not been studied before.

In the present work, it was found that lattice constant, bulk modulus, energy band gap and total magnetic moment are dependent directly with the concentration of V.

The major conclusions of this study can be summarized as follows:

1) The lattice parameter and bulk modulus for binary compounds AlP and VP are in good agreement with experimental results and other theoretical calculations.

2) The lattice parameter and bulk modulus are dependent on the concentration of doped V, such that the increasing in concentration of V decreases lattice parameter and increases bulk modulus.

zone integrations. Phys. Rev. B13, 5188-5192.

[49] Villars P., Calvert L.D. **Pearson's Handbook of Crystallographic Data for Intermetallic Phases**. American Society for Metals: Metals Park, Vol 1-3, 2nd ed., OH 44073, 1985.

[50] Murnaghan F.D. 1944. **The Compressibility of media under extreme pressure**. Proc. N. A. S. 30: 244-247.

[51] Denton A.R. and Ashcroft N.W. 1991. **Vegard's law**. Physical Review A 43 (6): 3161–3164.

[52] Slater J.C. 1964. **Atomic radii in crystals**. The Journal of Chemical Physics 41(10): 3199-3205.

[53] Lubarda V.A. 2003. **On the effective lattice parameter of binary alloys**. Mechanics of Materials 35: 53-68.

جامعة النجاح الوطنية

كلية الدراسات العليا

الخصائص الالكترونية والتركيبية والمغناطيسية للمخلوط الثلاثي $Al_{1-x}V_xP$ في حالة التركيب زنك بلند باستخدام طريقة الموجات المستوية المعدلة الخطية للجهد التام

إعداد

إيمان محمد عبد الحفيظ الرابي

إشراف

د. محمد سلامة سالم أبو جعفر

د.عبد الرحمن مصطفى أبو لبده

قدمت هذه الأطروحة استكمالا لمتطلبات درجة الماجستير في الفيزياء بكلية الدراسات العليا في جامعة النجاح الوطنية في نابلس – فلسطين.

2012

الخصائص الالكترونية والتركيبية والمغناطيسية للمخلوط الثلاثي $Al_{1-x}V_xP$ في حالة التركيب زنك بلند باستخدام طريقة الموجات المستوية المعدلة الخطية للجهد التام

إعداد

إيمان محمد عبد الحفيظ الرابي

إشراف

د.محمد سلامة سالم أبو جعفر

د. عبد الرحمن مصطفى أبو لبدة

الملخص

تم في هذه الأطروحة حساب الخصائص التركيبية والالكترونية والمغناطيسية للمخلوط الثلاثي $Al_{1-x}V_xP$ في حالة التركيب البلوري زنك بلند للتراكيز 0، 0.125، 0.25، 0.5، 0.75 و1 وذلك باستخدام طريقة الموجات المستوية المعدلة الخطية لجهد تام (FP-LAPW) المتطبق في برنامج(WIEN2k-code).

ولقد تم أيضا استخدام تقريب الكثافة المغزلية الموضعية (LSDA) ، وتقريب الميل الاتجاهي المعمم (GGA) للجهد التبادلي الترابطي.

لقد تم دراسة تطور البنية لحزم الطاقة والعزم المغناطيسي واعتمادها على ثابت الشبكة للمركب فوسفاد الألمنيوم AlP والمخلوط الثلاثي $Al_{1-x}V_xP$ وكانت النتائج جيدة بالمقارنة مع القيم العملية الحسابية الأخرى.

أظهرت الدراسة الحالية بأن المركب AlP شبه موصل وذو فجوة طاقةغير مباشرة مقدارها 1.6 الكترون فولت ولا يمتلك الخصائص المغناطيسية في التركيب البلوري الحالي.

وتبين أن $Al_{1-x}V_xP$ في تركيز 0.125 وجد أنه شبه موصل بفجوة طاقة غير مباشرة تقدر بحوالي 0.3 الكترون فولت .

للمخاليط الثلاثية $Al_{1-x}V_xP$ للتراكيز 0.25، 0.5 و 0.75 فجوة الطاقة لهم تساوي صفر مما يجعلهم فلزات أو أشباه فلزات. كما أن لهم عزم مغناطيسي يعتمد على تركيز عنصر الفاناديوم.أما بالنسبة للمركب VP فهو فلز وعزمه المغناطيسي 2 (μ_B) / وحده بناء .

ووجد أن ثابت الشبكة للمخاليط الثلاثية يعتمد على تركيز عنصر الفاناديوم.

قيمة العزم المغناطيسي وثابت الشبكة وفجوة الطاقة أكبر للتقريب GGA مقارنة مع LSDA ، أما بالنسبة لمعامل الصلابة فقيمته أكبر للتقريب LSDA مقارنة مع GGA .